School of Medicine and Faculty of Science
PH.D. PROGRAM IN TRANSLATIONAL AND MOLECULAR MEDICINE DIMET

Down Regulation of NLK by hsa-miR-221/222 Modulates Chemosensitivity to Glucocorticoids in Pediatric Normal Karyotype B-cell Precursor Acute Lymphoblastic Leukemia

Coordinator: Prof. Andrea Biondi
Tutors: Prof. Andrea Biondi, Dr. Giovanni Cazzaniga
PhD Candidate: Koh Thong Chuan Eugene
Matriculation No.: 0725284

XXIV CYCLE
ACADEMIC YEAR 2011-2012

格物致知

I dedicate this work to my parents and family, and Ailing.

Table of Contents

Chapter 3: Summary, Conclusions and Future Perspectives

Chapter 1 Introduction

1.1. Pediatric B-cell Precursor Acute Lymphoblastic Leukemia and its Pathogenesis

Acute Lymphoblastic Leukemia (ALL) is a malignancy of the B- or T-cell lymphoid system, and arises from a single lymphoblast that accumulates genetic abnormalities through the course of its maturation process[1,2]. These genetic abnormalities disrupt the normal maturation process by causing differentiation arrest, uncontrolled proliferation and increasing resistance to apoptotic signals that regulate survival of abnormal lymphoblasts. These abnormal lymphoblasts then proliferate at an accelerated rate, and in turn affect normal hematopoiesis by crowding out the growth of normal B- or T-cells.

ALL is a heterogeneous disease due to the whole spectrum of genetic abnormalities that can occur at any stage of the lymphoblast maturation process. The genetic abnormalities are primarily chromosomal translocations and secondary mutations that function synergistically with the former to effect leukemogenesis[1,2].

Chromosomal translocations result in fusion genes that produce impaired or oncogenic proteins. An example is the t(9;22) which forms the BCR-ABL fusion gene that produces a constitutive tyrosine kinase that is hyperactive and excessively activates the

RAS[3], JAK-STAT[4] and MAPK[5] pathways that serve to increase anti-apoptotic activity, proliferation and survival.

Other than producing oncogenic kinase fusion proteins, chromosomal translocations can also result in chimeric transcription factors. One good example is the t(12;21) translocation that forms the TEL-AML1 fusion protein. Normal AML1 binds to DNA with the recruitment of histone acetylases and cotransactivators to initiate transcription of genes required for normal hematopoiesis[6]. However, while TEL-AML1 retains the DNA binding capability, it now recruits histone deacetylases that changes the chromatin conformation to inhibit transcription[7]. This transcription inhibition then interferes with normal progenitor cell differentiation and survival.

Secondary mutations that result in excessive gene expression or repression, mediated by hyper/hypoploidy or gene duplication/deletion respectively, functions synergistically with the activity of fusion proteins to promote leukemogenesis. Examples are FLT-3 receptor over expression and deletion of INK4 genes in the Retinoblastoma pathway. Excessive FLT-3 receptors result in continuous FLT-3 tyrosine kinase activity[8,9] that induces excessive cell growth, while the loss of INK4 genes prevents the retinoblastoma protein from suppressing cellular proliferation[10].

The stage at which differentiation is arrested further classifies the disease into Pre-pre-B, Common, Pre-B, Pre-T, Early-T, Intermediate-T or Mature-T ALL. B-cell precursor ALL (BCP-ALL) accounts for 80-85% of all ALL cases while the T-cell lineage accounts for the remaining percentages.[1,2]

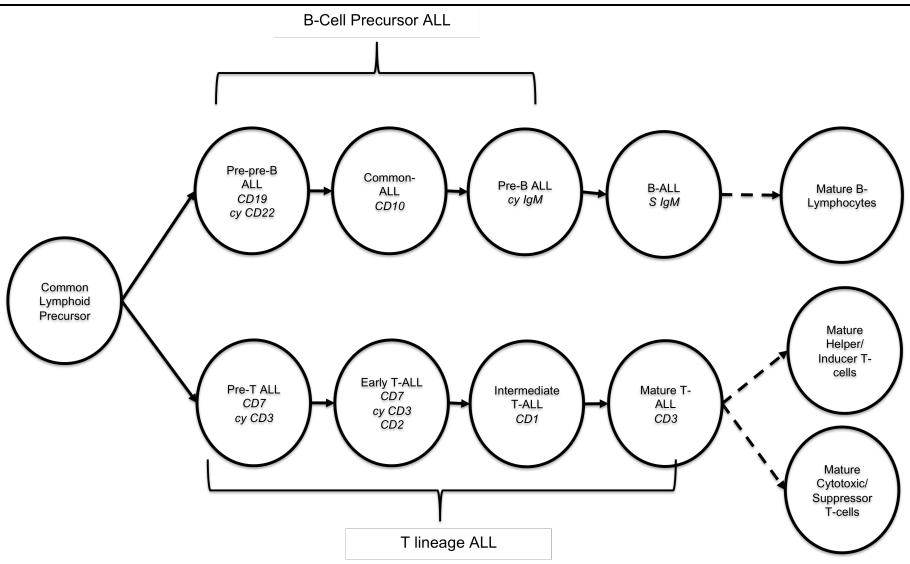

Figure 1. ALL subtypes distribution in the lymphoblast maturation process. Antigens required for distinct stage definition are shown in italics.

A.

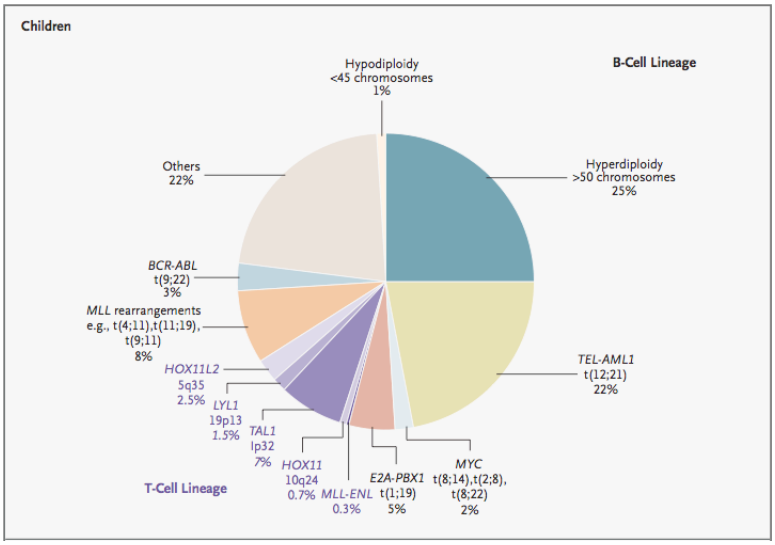

B.

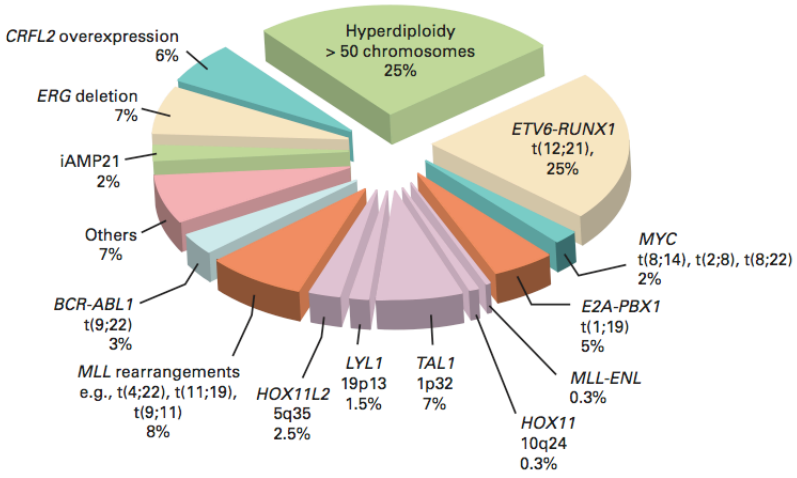

Figure 2. Estimated frequency of ALL subtypes in children. A. 2004 estimates[2]. **B.** 2011 estimates[11].

As summarized by Pui[11] et al, ALL pathogenesis is mainly a result of genetic lesions, however, there is a subset of patients who do not exhibit any of these genetic lesions, and still develop the disease. Previously, 22%[2] of ALL patients fall into this 'Others' category and the figures were recently revised downwards to 7%[11]. These patients classified in the 'Others' category are termed Normal Karyotype (NK) as they do not exhibit known cytogenetic abnormalities and are heterogeneous in their responses to chemotherapy and relapse rates.

For the purposes of this thesis, the focus is on pediatric NK BCP-ALL patients.

1.2. Minimal Residual Disease and its Measurement

In this study, patient samples were obtained from the AIEOP-BFM ALL 2000 project.

Currently, all leukemia patients enrolled in the AIEOP-BFM ALL protocol are stratified according to minimal residual disease (MRD) measurements at induction and consolidation treatment time points into Standard Risk, Intermediate Risk and High Risk groups, representing 42.6%, 42.6% and 14.8% of all patients assessed[12]. Within these 3 groups, the 5-year relapse rates were 2%, 22% and 80% respectively. MRD measurement procedure involves the

detection and monitoring of immunoglobulin and T-cell receptor (TCR) gene rearrangements through quantitative real-time PCR (qRT-PCR)[13,14]. This procedure has high sensitivity, capable of detecting 1 leukemic cell out of $1X10^4$-$1X10^5$ normal cells[15]. It had been shown in previous studies[16,17,18] that outcome prediction is greatly improved by early MRD detection during chemotherapy initiation. Hence, these observations underscore the value of MRD measurements in optimizing patient treatments.

1.3. Significance of Normal Karyotype Acute Lymphoblastic Leukemia

Among patients' subgroups defined by chromosomal genetic markers, t(12;21) positive patients have good prognostic indication, as well as hyperdiploids. Vice versa, t(9;22) and t(4;11) positive patients have poor prognosis.

On the contrary, patients with normal karyotypes exhibit differential responses to chemotherapy, due to unknown causes. In order to prescribe effective follow-up treatment for patients with refractory responses and improve on patient survival rates, there must be more information about the mechanism of resistance in normal karyotype patients. Furthermore, the heterogeneity of these patients in response to chemotherapy as measured by MRD suggests an underlying important variable or factor that determines chemotherapy response and relapse rates; hence the study of

these patients will provide additional biological insights and further understanding of chemoresistance and relapse.

Therefore an objective is to identify miRNA markers that segregate Normal Karyotype patients into their respective MRD risk categories, and evaluate if the miRNAs are responsible for modulating chemoresistance.

1.4. Implications of miRNA in oncogenesis

miRNAs are a class of non-coding RNAs that regulate gene expression through post-transcriptional control, by incomplete complementary base pairing with their target mRNAs to disrupt translation and/or initiate mRNA degradation[19]. miRNAs had been identified as important factors in leukemogenesis initiation, progression and resistance to chemotherapy, examples are miR-15/16[20], miR-29b[21], miR-181b[22], miR-125b[23] and miR-221/222[24,25,26,27]. Here, it is proposed to investigate whether miRNAs are differentially expressed among NK BCP-ALL patients with different MRD prognostic groups and in this way provide insights about mechanisms of chemotherapy resistance and relapse in this subset of ALL.

1.6. Scope of the study

This study aims to determine if miRNAs are differentially expressed between Standard Risk (SR) and non-Standard Risk (inclusive of Intermediate Risk, IR and High Risk HR) pediatric NK BCP-ALL patients, identify the associated protein and perform functional analyses to validate their roles in chemoresistance. For clarity and accuracy in nomenclature, SR patients are termed MRD Low (ML) while HR and IR patients are termed MRD High (MH).

Chapter 2.

2.1. Materials and Methods

2.1.1. Patient Samples

Patient RNA samples were obtained from the AIEOP-BFM ALL 2000 study and were used for subsequent Low Density Array (AppliedBiosystems) and TAQMAN miRNA Single Assay analyses.

2.1.2. TaqMan® Human miRNA Arrays

RNA samples were reverse transcribed using TaqMan® miRNA Reverse Transcription Kit (Applied Biosystems) and Megaplex™ RT primers pool A and B (Applied Biosystems). A 1X RT reaction mix was made up of 0.8uL 10X Megaplex™ RT primers, 0.2uL of 100mM dNTPs with dTTPs, 1.5uL 50U/uL Multiscribe Reverse Transcriptase, 0.8uL 10X RT buffer, 0.9uL 25mM $MgCl_2$, 0.1uL 20U/uL RNase inhibitor and 0.2uL of nuclease-free water. 3uL of total RNA was added to 4.5uL of RT mix and was incubated on ice for 5min before being loaded onto a thermocycler running 40 cycles of 16°C for 2min, 42°C for 1min, 50°C for 1sec, followed by 85°C for 5min to denature the Multiscribe Reverse Transcriptase, and a final hold at 4°C. Thereafter, the cDNA samples were amplified using Megaplex™ PreAmp primers (AppliedBiosystems, Carlsbad, CA.) before being loaded into the respective TaqMan® Human MicroRNA Array Card A & B v2 (4400238,

AppliedBiosystems, Carlsbad, CA.) for qRT-PCR quantification. The 1X PreAmp reaction mix was made up of 12.5uL 2X Taqman® PreAmp Master Mix, 2.5uL 10X Megaplex™ PreAmp primers and 7.5uL of nuclease free water. For each sample, 2.5uL of RT product was added to 22.5uL of PreAmp reaction mix and allowed to incubate on ice for 5min before loaded onto a thermocycler running 95°C for 10min, 55°C for 2min, 72°C for 2min, followed by 12 cycles of 95°C for 15sec and 60°C for 4min, followed by 99.9°C for 10min and a final hold of 4°C. The amplified samples were each diluted with 75ul of 0.1X TE pH 8.0. The 1X qRT-PCR mix was made up of 450uL 2X TaqMan Universal PCR Master Mix No AmpErase® UNG, 441uL of nuclease-free water and 9uL of diluted PreAmp product. The loaded array cards were run in 7900HT sequence detector (AppliedBiosystems, Carlsbad, CA.) running at 95°C for 10min and 40cycles of 95°C for 15sec and 60°C for 1min. Excel spreadsheet was used in calculating DCt values that were normalized to RNU48 expression levels. Gene Cluster 3.0 was used to perform clustering analysis. The data was filtered for 100% expression in all patient samples; log transformed, centered on the median expression data and normalized across all samples. For unsupervised clustering of miRNAs and patient samples, average linkage and un-centered correlation algorithm was used. The resultant heatmaps were plotted using Java TreeView version 1.1.6.

2.1.3. Taqman miRNA Expression Assay

Total RNA samples were reverse transcribed using the TaqMan MicroRNA Reverse Transcription Kit and the specific primers for RNU48, hsa-let-7e, hsa-miR-21, hsa-miR-221, hsa-miR-222, hsa-miR-24, hsa-miR-29a, hsa-miR-30b (AppliedBiosystems Assay IDs: 001006, 002406, 000397, 000524, 002276, 000402, 002112, 00602). The 1X reverse transcription mix was composed of 0.15uL 100mM dNTP with dTTP, 1uL Multiscribe Reverse Transcriptase 50U/uL, 1.5uL 10X reverse transcription buffer, 0.19uL RNAse inhibitor 20U/uL and 4.16uL of nuclease free water, 3uL of 5X specific miRNA reverse transcription primers, and 5uL of sample RNA, making a total volume of 15uL, and was subject to the thermocycler routine of 16°C for 30min, 42°C for 30min, 85°C for 5min and a final holding temperature of 21°C. The resultant cDNA were quantified in qRT-PCR with the supplied probes for each miRNA assay.

2.1.4. Taqman Gene Expression Assay

Total RNA samples were reverse transcribed using the High Capacity cDNA Reverse Transcription Kit. The 1X reverse transcription mix was made up of 2ul 10X reverse transcription buffer, 0.8ul 25X 100mM dNTP mix, 2ul 10X reverse transcription random primers, 1ul Multiscribe Reverse Transcriptase, 4.2ul of nuclease free water and 10ul of total RNA making a total volume of 20ul, and was subject to the thermocycler routine of 25°C for

10min, 37°C for 120min, 85°C for 5min and a final holding temperature of 21°C. The resultant cDNA were quantified in qRT-PCR with probes for Nemo-Like Kinase (AppliedBiosystems ID: Hs00212076_m1) and normalized to GAPDH (AppliedBiosystems ID: Hs02758991_g1). For both miRNA and Gene Expression assays, the 1X qRT-PCR mix was made up of 1ul 20X Assay primers, 10ul 2X TaqMan® Universal PCR Master Mix No AmpErase UNG, 8ul nuclease free water and 1ul of cDNA, total volume 20ul. The reaction mixes were subjected to the thermocycler routine of 50°C for 2min, 95°C for 10min and 40cycles of 95°C for 15sec and 60°C for 1min in AB7900HT (AppliedBiosystems, Carlsbad. CA.).

2.1.5. Screening Cell Lines for Glucocorticoid Sensitivity

The pre-cursor B-cell cell lines 380 (DSMZ ACC no.39) 697 (DSMZ ACC no.42) and SEM (DSMZ ACC no.546) were obtained from the German Collection of Microorganisms and Cell Cultures (Deutsche Sammlung von Mikroorganismen und Zellkulturen (DSMZ) GmbH, Braunschweig, Germany).

For initial screening of cell lines for drug sensitivity, cells were seeded at 1E6/mL, 100uL final volume, in 96 well plates. Drugs were diluted in RPMI at 100uM, 10uM, 1uM and 0.1uM before use. 1uL of drug of each concentration was added to each well to obtain final concentrations of 1uM, 0.1uM, 0.01uM and 0.001uM

respectively. The procedure was reported in triplicates, and cells were allowed to incubate for 72hrs at 37°C, 5% CO2 atmosphere before being assayed with CellTitreGlo (Promega, Madison WI).

A.

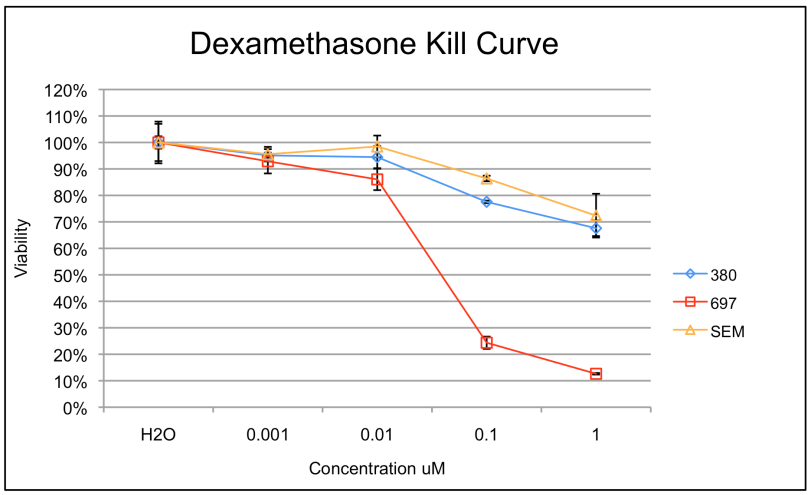

B.

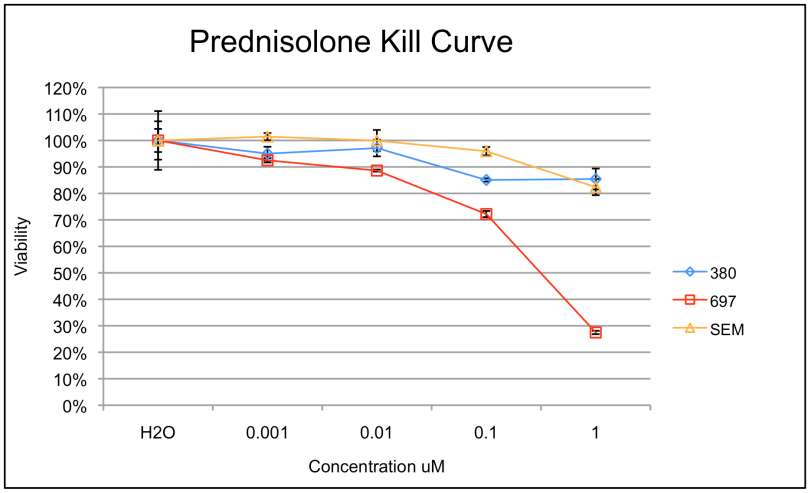

Figure 3. Dexamethasone and Prednisolone kill curves identifying 697 as the glucocorticoid sensitive cell line. For 697 cell line, Dexamethasone(LD50=0.05uM) is ~10fold more cytotoxic than Prednisolone (LD50=0.5uM).

In order to simplify experimental procedures, final concentrations of 0uM, 0.32uM, 0.64uM and 0uM, 0.08uM, 0.16uM were used for subsequent Prednisolone and Dexamethasone treatment assays respectively.

2.1.6. Stable Cell Line Construction

Lentiviral technology from System Biosciences (CA, USA) was used in the construction of the stable cell lines overexpressing miRNAs. Using EcoRI (New England Biolabs) and NotI (New England Biolabs), the pre-miR fragment was excised from the pMIRNA1 backbone. Using the T4 DNA Ligase (New England Biolabs) the required fragments were ligated into pCDH-MSCV-MCS-EF1-GFP-PURO (catalog no.CD713B-1) vector. The pseudo-viral particles were packaged in HEK293TN cells grown to ~80% confluency in T175 flasks, and the viral packaging mix was composed of 1mL serum-free DMEM, 45uL of pPACKH1, 4.5ug of lentivector construct and 55uL of Purefection. The packaging mix was incubated at room temperature for 15min before adding 40mL of DMEM supplemented with 10% Fetal Bovine Serum. Old media was aspirated from the T175 flasks and replaced with the packaging mix diluted in DMEM+10%FBS. The cells were left to incubate at 37°C with 5% CO_2 atmosphere for 72hrs. To harvest pseudo-viral particles, the supernatant was aspirated into 50mL Falcon tubes and centrifuged at 3000X g for 15min to pellet the cell debris. The viral supernatant was transferred to a new 50mL

Falcon tube and 1 volume of cold (4°C) PEG-it Virus Precipitation Solution was added to every 4 volumes of viral supernatant and refrigerated at 4°C for more than 12hrs to pellet the viral particles. After refrigeration, the viral supernatant mix was centrifuged at 1500X g for 30min at 4°C. The supernatant was aspirated and the precipitated pellet was re-suspended in 4mL of RPMI. For transfection, 1mL of viral particles was added to 4mL of 5e6 cells and supplemented with 25uL of Transdux reagent. CoGFP fluorescence was observed 72hr post transfection, and cells were subject to Puromycin selection for 2 passages at a concentration of 0.3ug/ml.

2.1.7. 697 Cell Line Optimization & Transient Transfection

A1.

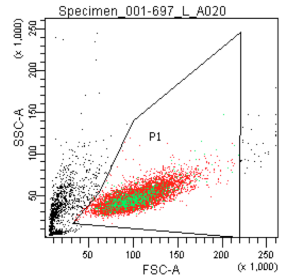

Tube: 697_L_A020

Population	#Events	%Parent	%Total
All Events	11,624	####	100.0
P1	9,987	85.9	85.9
P2	626	6.3	5.4
P3	655	6.6	5.6

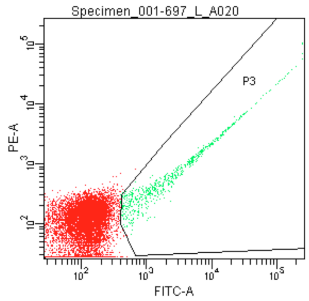

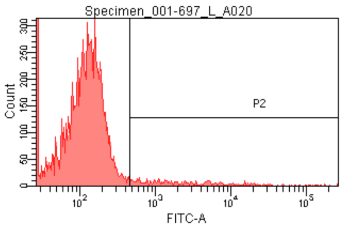

A2.

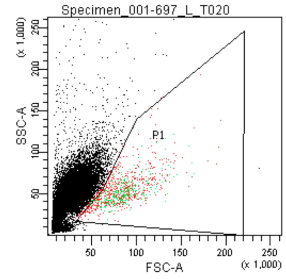

Tube: 697_L_T020

Population	#Events	%Parent	%Total
All Events	18,700	####	100.0
P1	951	5.1	5.1
P2	279	29.3	1.5
P3	281	29.5	1.5

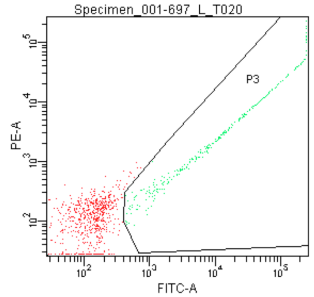

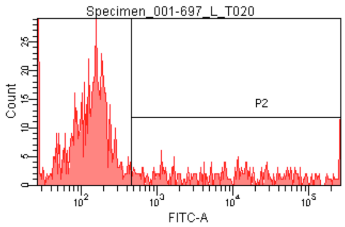

A3.

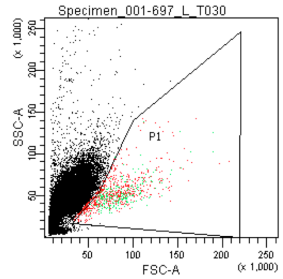

Tube: 697_L_T030

Population	#Events	%Parent	%Total
All Events	20,162	####	100.0
P1	867	4.3	4.3
P2	224	25.8	1.1
P3	229	26.4	1.1

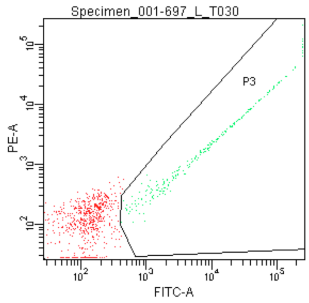

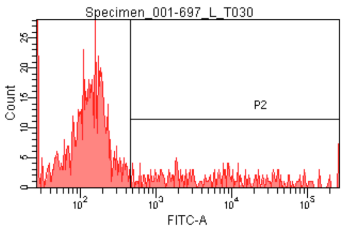

A4.

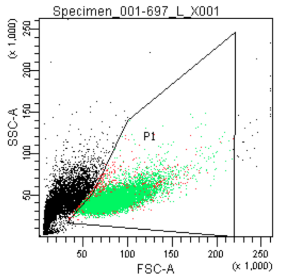

Tube: 697_L_X001

Population	#Events	%Parent	%Total
All Events	16,104	####	100.0
P1	9,811	60.9	60.9
P2	7,115	72.5	44.2
P3	7,132	72.7	44.3

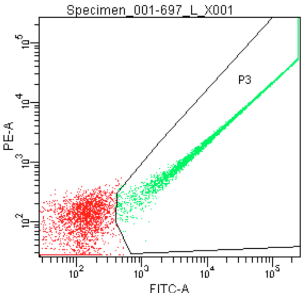

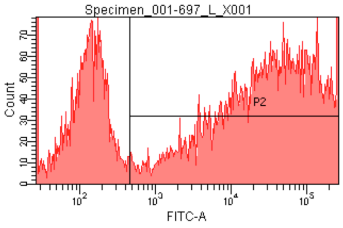

A5.

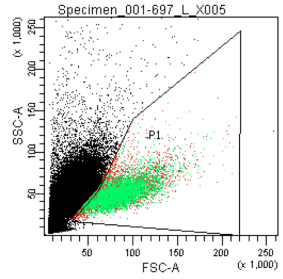

Tube: 697_L_X005

Population	#Events	%Parent	%Total
All Events	57,426	####	100.0
P1	9,189	16.0	16.0
P2	4,939	53.7	8.6
P3	4,963	54.0	8.6

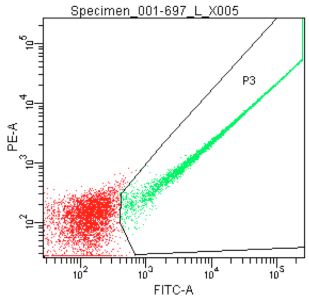

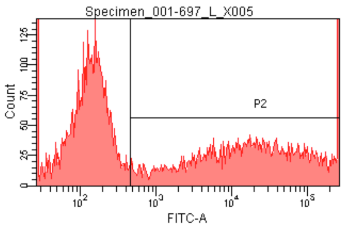

A6.

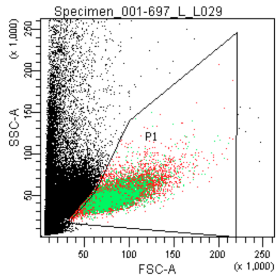

Tube: 697_L_L029

Population	#Events	%Parent	%Total
All Events	48,484	####	100.0
P1	9,623	19.8	19.8
P2	2,809	29.2	5.8
P3	2,855	29.7	5.9

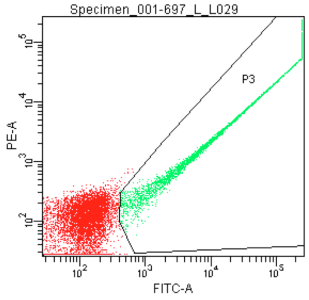

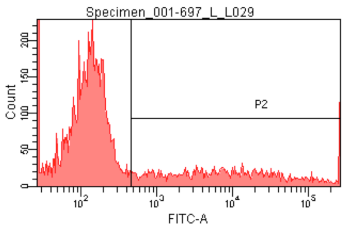

A7.

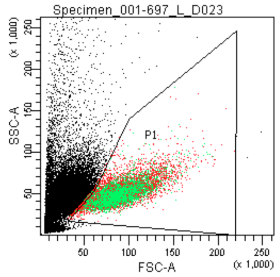

Tube: 697_L_D023

Population	#Events	%Parent	%Total
All Events	31,641	####	100.0
P1	8,289	26.2	26.2
P2	2,335	28.2	7.4
P3	2,365	28.5	7.5

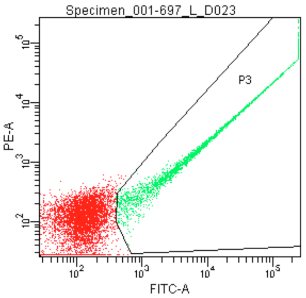

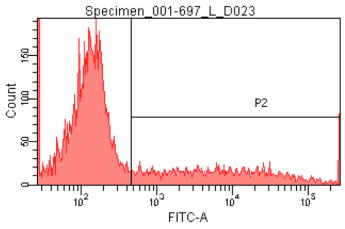

A8.

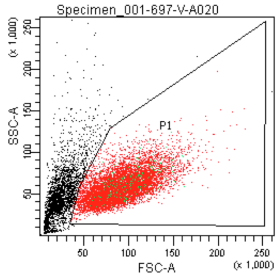

Tube: 697-V-A020

Population	#Events	%Parent	%Total
All Events	12,578	####	100.0
P1	9,732	77.4	77.4
P2	206	2.1	1.6
P3	190	2.0	1.5

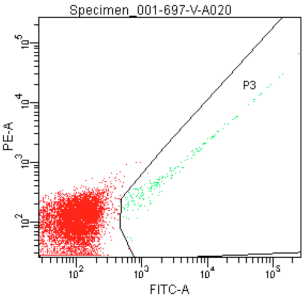

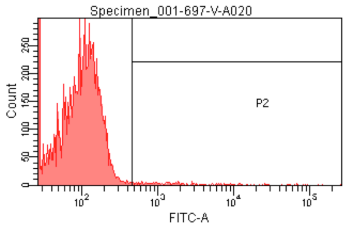

A9.

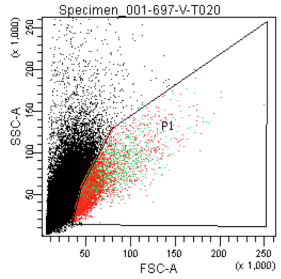

Tube: 697-V-T020

Population	#Events	%Parent	%Total
All Events	83,097	####	100.0
P1	10,000	12.0	12.0
P2	663	6.6	0.8
P3	616	6.2	0.7

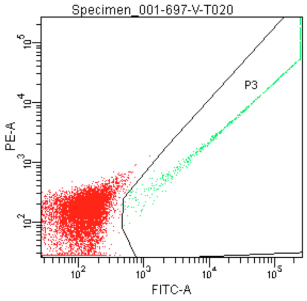

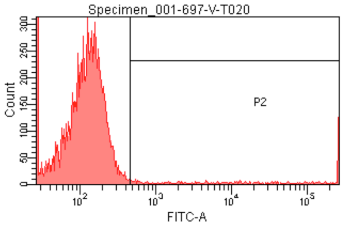

A10.

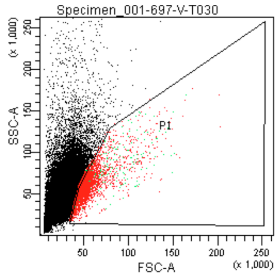

Tube: 697-V-T030

Population	#Events	%Parent	%Total
All Events	59,014	####	100.0
P1	3,710	6.3	6.3
P2	159	4.3	0.3
P3	143	3.9	0.2

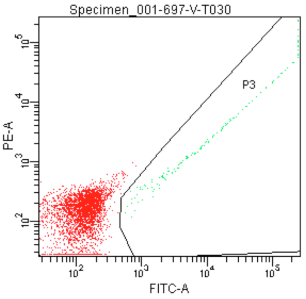

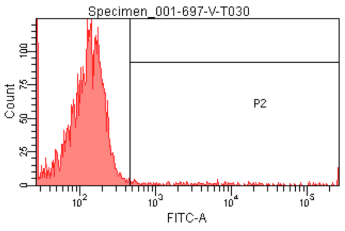

A11.

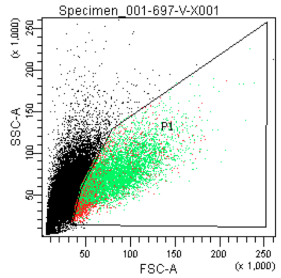

Tube: 697-V-X001

Population	#Events	%Parent	%Total
All Events	38,465	####	100.0
P1	10,000	26.0	26.0
P2	4,709	47.1	12.2
P3	4,658	46.6	12.1

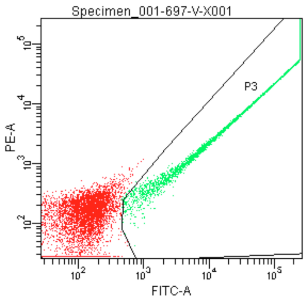

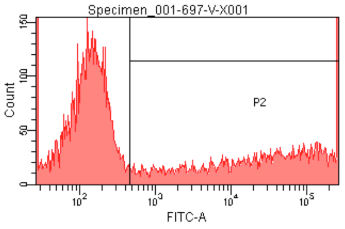

A12.

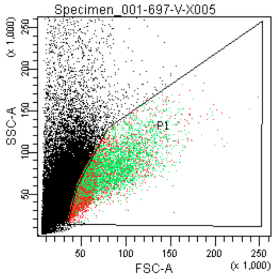

Tube: 697-V-X005

Population	#Events	%Parent	%Total
All Events	73,886	####	100.0
P1	10,000	13.5	13.5
P2	2,709	27.1	3.7
P3	2,657	26.6	3.6

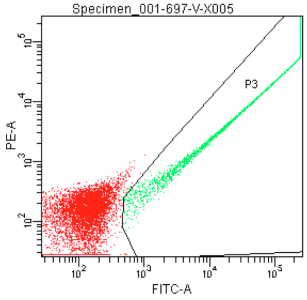

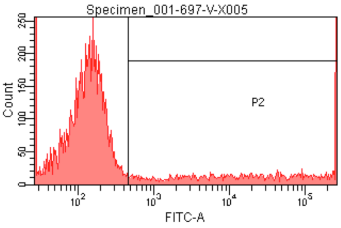

A13.

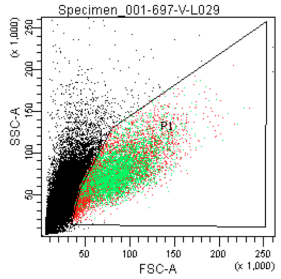

Tube: 697-V-L029

Population	#Events	%Parent	%Total
All Events	41,426	####	100.0
P1	10,000	24.1	24.1
P2	3,700	37.0	8.9
P3	3,663	36.6	8.8

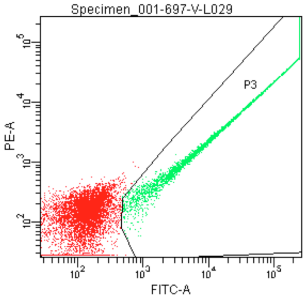

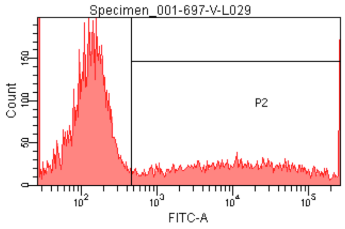

A14.

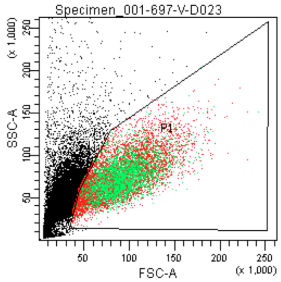

Tube: 697-V-D023

Population	#Events	%Parent	%Total
All Events	25,977	####	100.0
P1	10,000	38.5	38.5
P2	2,965	29.6	11.4
P3	2,910	29.1	11.2

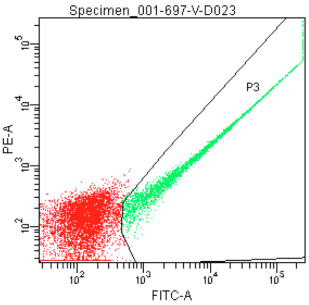

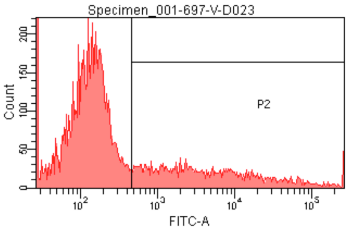

B1.

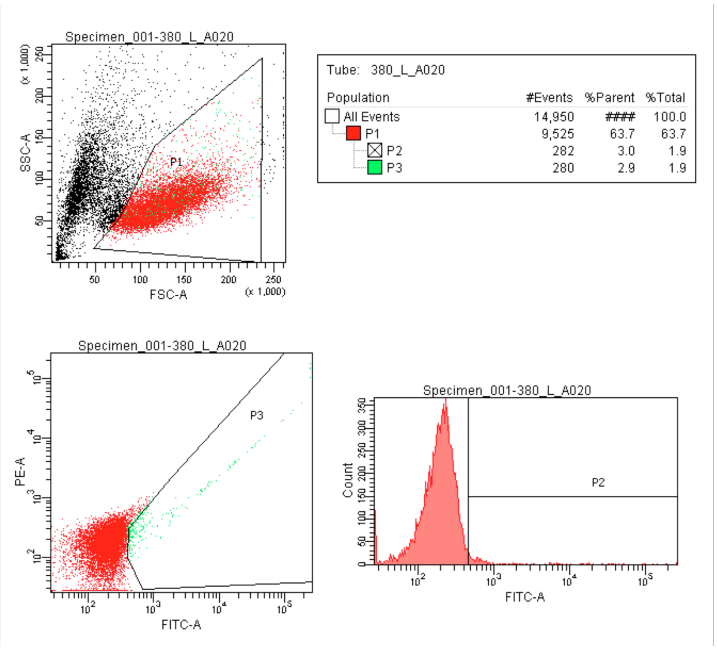
Specimen_001-380_L_A020
SSC-A
FSC-A
P1
Tube: 380_L_A020
Population #Events %Parent %Total
All Events 14,950 #### 100.0
P1 9,525 63.7 63.7
P2 282 3.0 1.9
P3 280 2.9 1.9
Specimen_001-380_L_A020
PE-A
FITC-A
P3
Specimen_001-380_L_A020
Count
FITC-A
P2

B2.

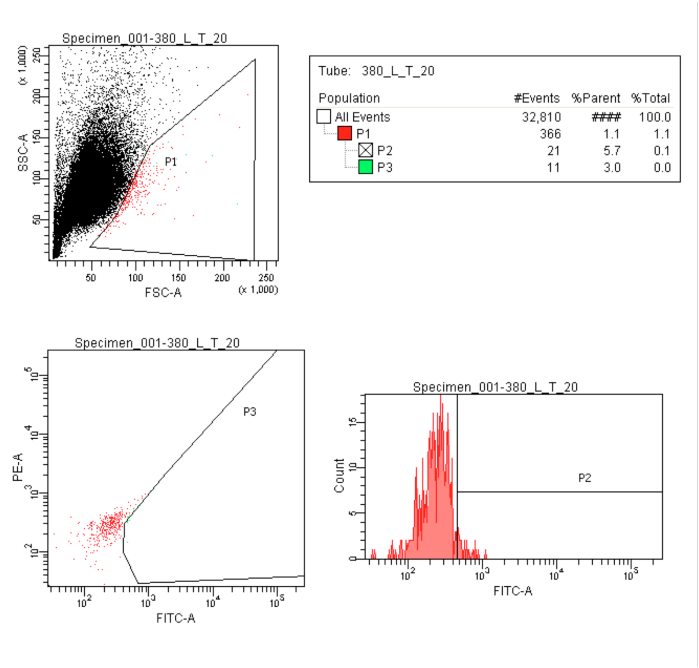
Specimen_001-380_L_T_20
SSC-A
FSC-A
P1
Tube: 380_L_T_20
Population #Events %Parent %Total
All Events 32,810 #### 100.0
P1 366 1.1 1.1
P2 21 5.7 0.1
P3 11 3.0 0.0
Specimen_001-380_L_T_20
PE-A
FITC-A
P3
Specimen_001-380_L_T_20
Count
FITC-A
P2

B3.

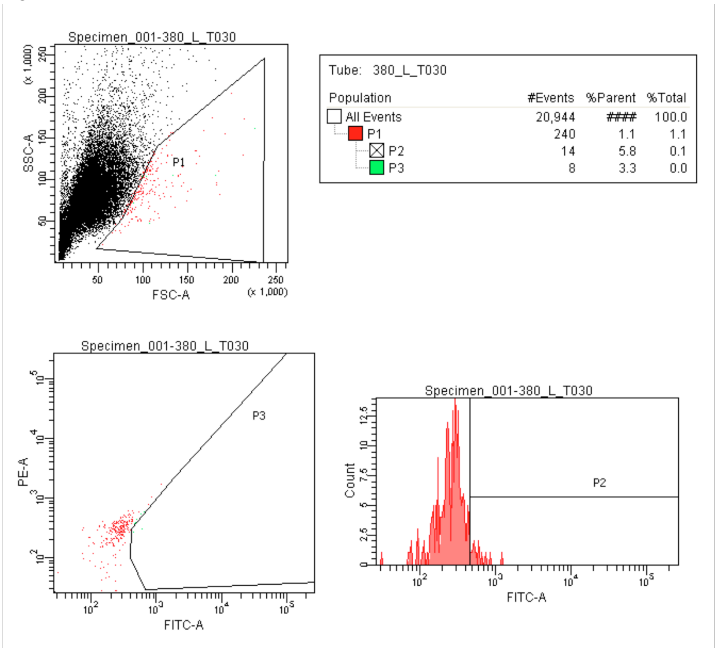
Specimen_001-380_L_T030
SSC-A
FSC-A
P1
Tube: 380_L_T030
Population #Events %Parent %Total
All Events 20,944 #### 100.0
P1 240 1.1 1.1
P2 14 5.8 0.1
P3 8 3.3 0.0
Specimen_001-380_L_T030
PE-A
FITC-A
P3
Specimen_001-380_L_T030
Count
FITC-A
P2

B4.

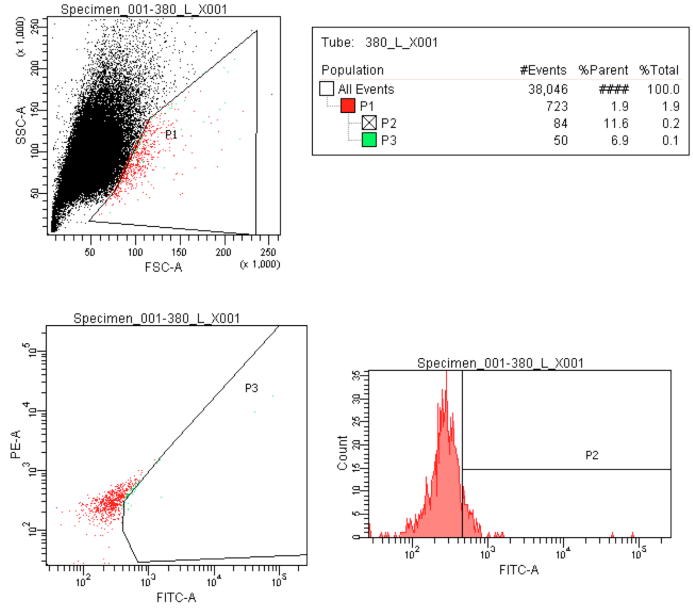
Specimen_001-380_L_X001
SSC-A
FSC-A
P1
Tube: 380_L_X001
Population #Events %Parent %Total
All Events 38,046 #### 100.0
P1 723 1.9 1.9
P2 84 11.6 0.2
P3 50 6.9 0.1
Specimen_001-380_L_X001
PE-A
FITC-A
P3
Specimen_001-380_L_X001
Count
FITC-A
P2

B5.

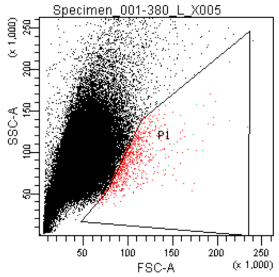

Tube: 380_L_X005

Population	#Events	%Parent	%Total
All Events	65,671	####	100.0
P1	830	1.3	1.3
P2	53	6.4	0.1
P3	30	3.6	0.0

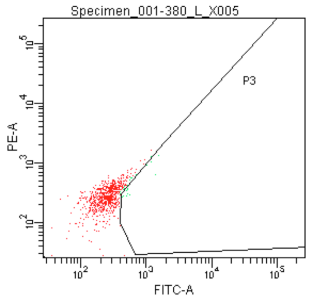

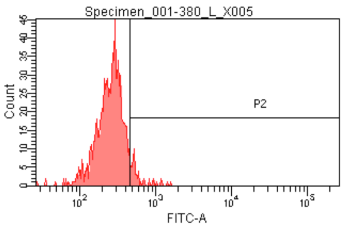

B6.

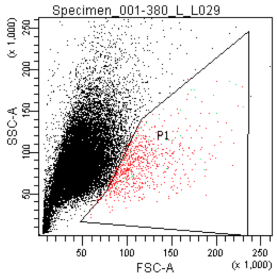

Tube: 380_L_L029

Population	#Events	%Parent	%Total
All Events	22,678	####	100.0
P1	814	3.6	3.6
P2	74	9.1	0.3
P3	38	4.7	0.2

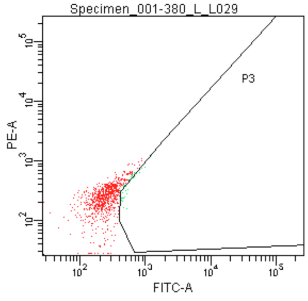

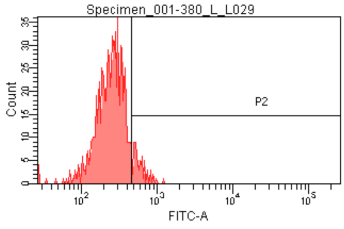

B7.

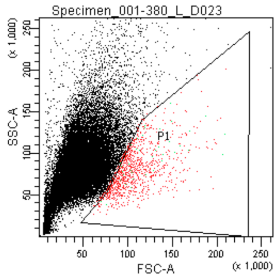

Tube: 380_L_D023			
Population	#Events	%Parent	%Total
All Events	30,667	####	100.0
P1	1,008	3.3	3.3
P2	106	10.5	0.3
P3	44	4.4	0.1

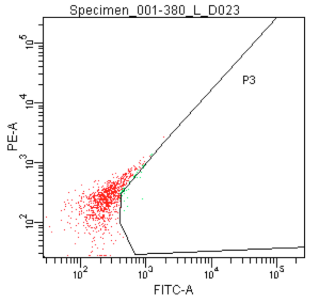

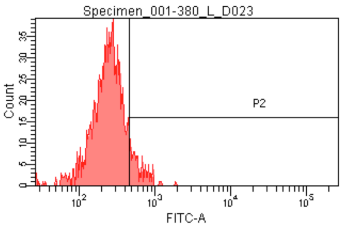

B8.

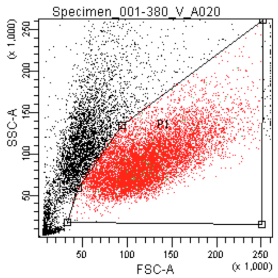

Tube: 380_V_A020			
Population	#Events	%Parent	%Total
All Events	15,624	####	100.0
P1	9,757	62.4	62.4
P2	246	2.5	1.6
P3	121	1.2	0.8

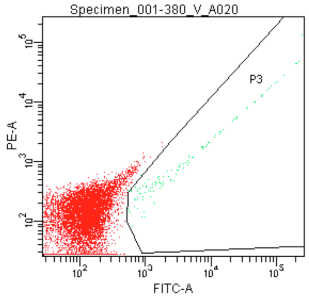

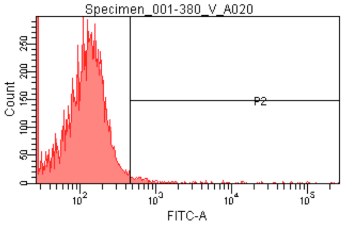

B9.

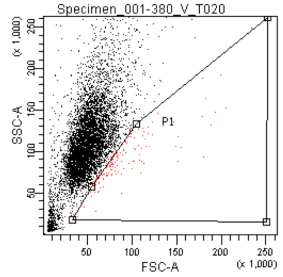

Tube: 380_V_T020			
Population	#Events	%Parent	%Total
All Events	7,123	####	100.0
P1	164	2.3	2.3
P2	3	1.8	0.0
P3	0	0.0	0.0

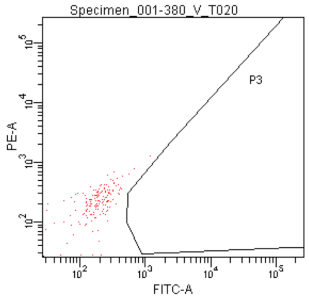

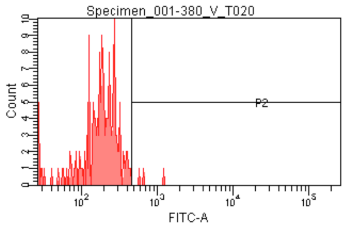

B10.

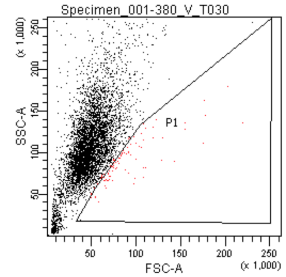

Tube: 380_V_T030			
Population	#Events	%Parent	%Total
All Events	5,559	####	100.0
P1	106	1.9	1.9
P2	8	7.5	0.1
P3	0	0.0	0.0

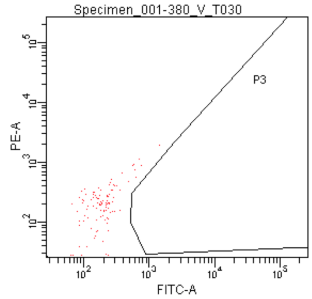

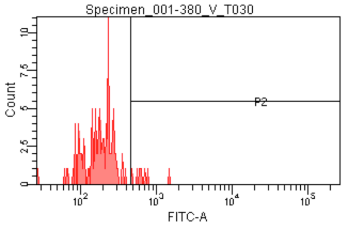

B11.

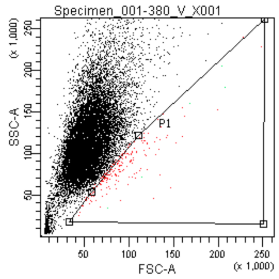

Tube: 380_V_X001

Population	#Events	%Parent	%Total
All Events	15,096	####	100.0
P1	203	1.3	1.3
P2	18	8.9	0.1
P3	5	2.5	0.0

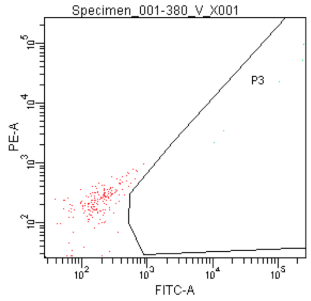

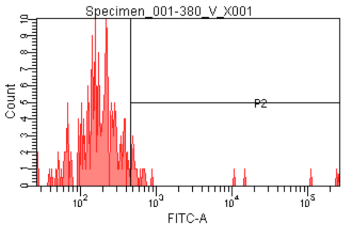

B12.

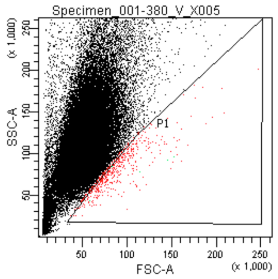

Tube: 380_V_X005

Population	#Events	%Parent	%Total
All Events	62,458	####	100.0
P1	511	0.8	0.8
P2	51	10.0	0.1
P3	5	1.0	0.0

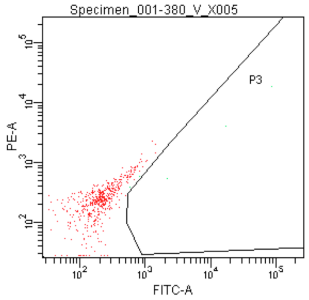

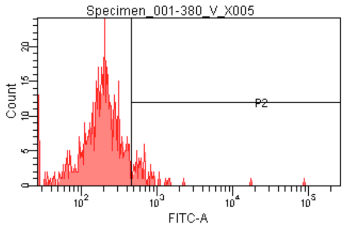

B13.

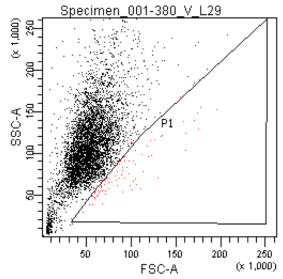

Tube: 380_V_L29			
Population	#Events	%Parent	%Total
All Events	5,542	####	100.0
P1	102	1.8	1.8
P2	9	8.8	0.2
P3	1	1.0	0.0

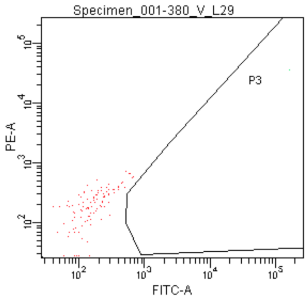

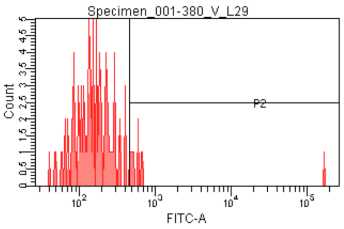

B14.

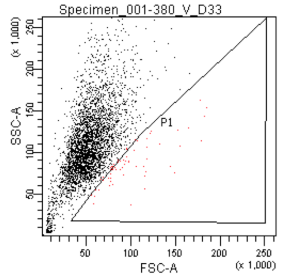

Tube: 380_V_D33			
Population	#Events	%Parent	%Total
All Events	3,723	####	100.0
P1	66	1.8	1.8
P2	8	12.1	0.2
P3	0	0.0	0.0

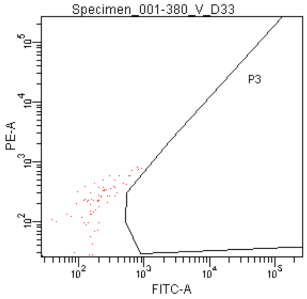

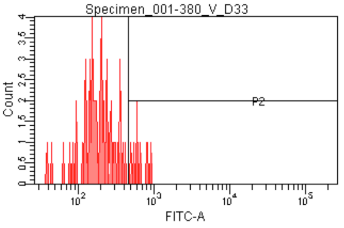

C1.

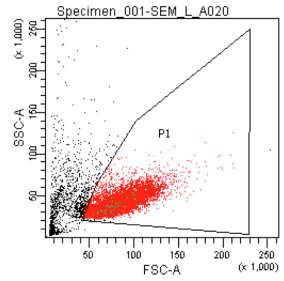

Tube: SEM_L_A020			
Population	#Events	%Parent	%Total
All Events	10,929	####	100.0
P1	9,523	87.1	87.1
P2	56	0.6	0.5
P3	61	0.6	0.6

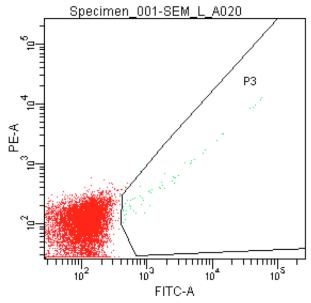

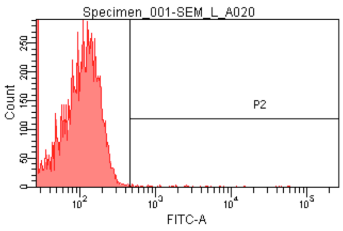

C2.

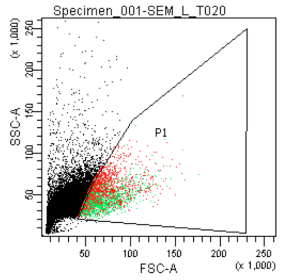

Tube: SEM_L_T020			
Population	#Events	%Parent	%Total
All Events	15,682	####	100.0
P1	3,111	19.8	19.8
P2	716	23.0	4.6
P3	729	23.4	4.6

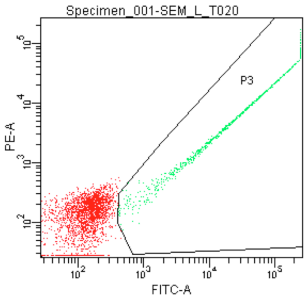

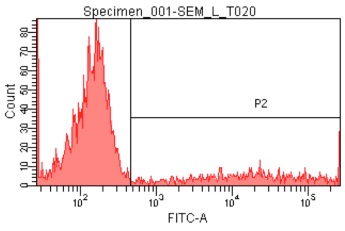

C3.

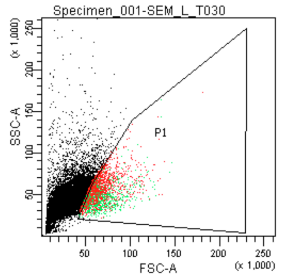

Tube: SEM_L_T030

Population	#Events	%Parent	%Total
All Events	16,215	####	100.0
P1	2,481	15.3	15.3
P2	449	18.1	2.8
P3	458	18.5	2.8

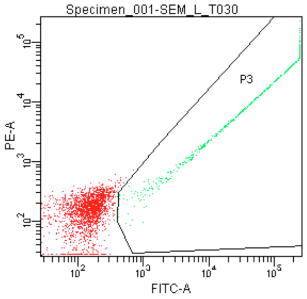

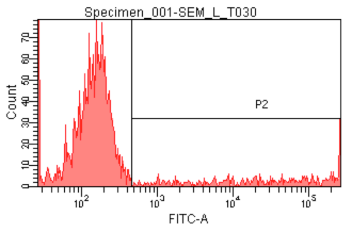

C4.

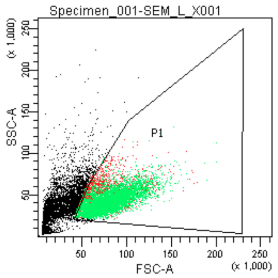

Tube: SEM_L_X001

Population	#Events	%Parent	%Total
All Events	12,243	####	100.0
P1	7,880	64.4	64.4
P2	5,591	71.0	45.7
P3	5,608	71.2	45.8

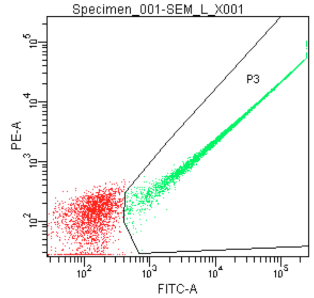

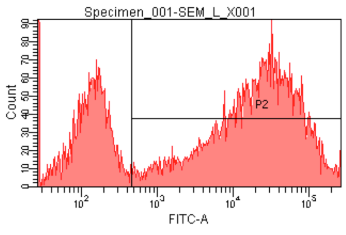

C5.

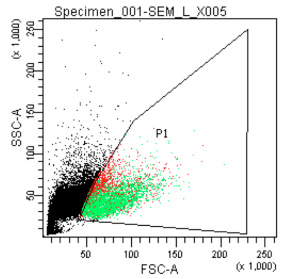

Tube: SEM_L_X005

Population	#Events	%Parent	%Total
All Events	14,096	####	100.0
P1	4,802	34.1	34.1
P2	2,478	51.6	17.6
P3	2,496	52.0	17.7

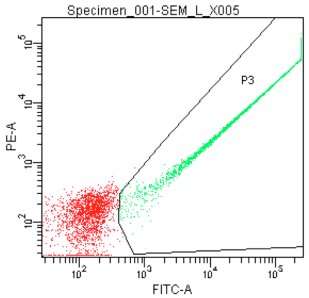

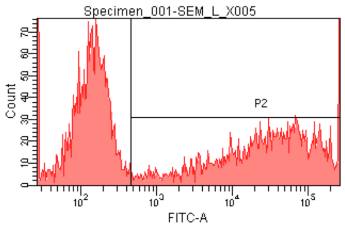

C6.

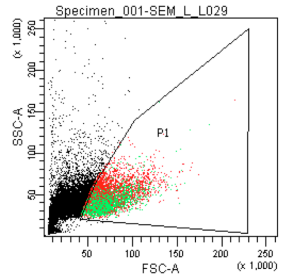

Tube: SEM_L_L029

Population	#Events	%Parent	%Total
All Events	14,318	####	100.0
P1	5,243	36.6	36.6
P2	1,157	22.1	8.1
P3	1,172	22.4	8.2

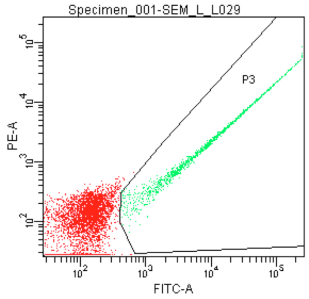

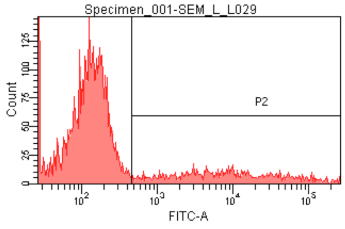

C7.

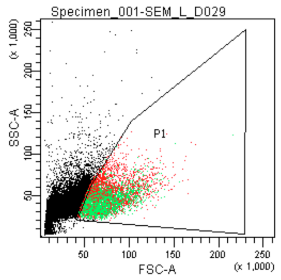

Tube: SEM_L_D029			
Population	#Events	%Parent	%Total
All Events	14,549	####	100.0
P1	5,381	37.0	37.0
P2	1,439	26.7	9.9
P3	1,458	27.1	10.0

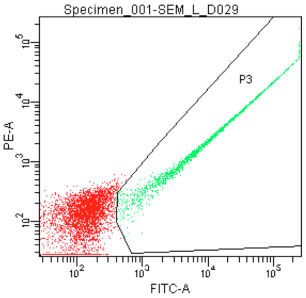

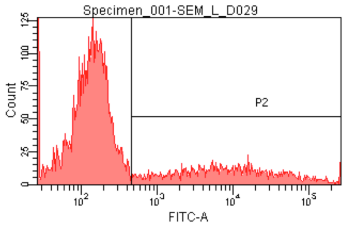

C8.

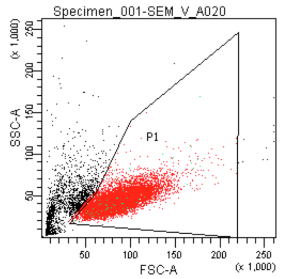

Tube: SEM_V_A020			
Population	#Events	%Parent	%Total
All Events	10,987	####	100.0
P1	9,304	84.7	84.7
P2	54	0.6	0.5
P3	56	0.6	0.5

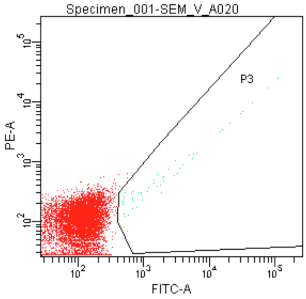

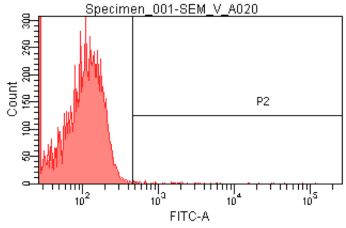

C9.

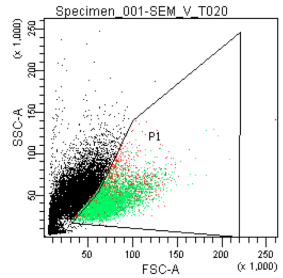

Tube: SEM_V_T020

Population	#Events	%Parent	%Total
All Events	14,454	####	100.0
P1	5,468	37.8	37.8
P2	3,814	69.8	26.4
P3	3,828	70.0	26.5

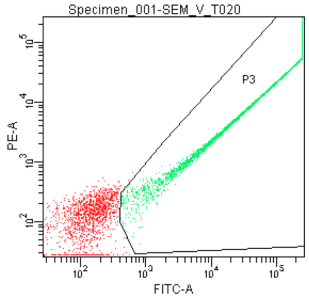

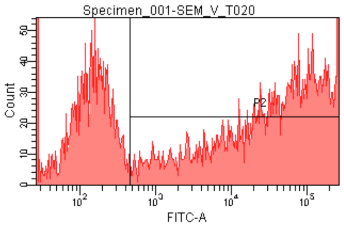

C10.

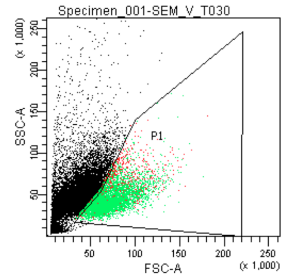

Tube: SEM_V_T030

Population	#Events	%Parent	%Total
All Events	15,606	####	100.0
P1	5,094	32.6	32.6
P2	3,494	68.6	22.4
P3	3,509	68.9	22.5

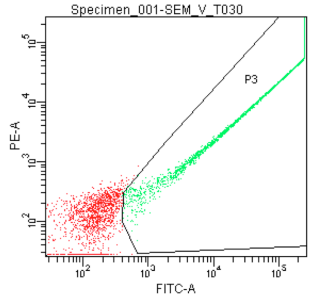

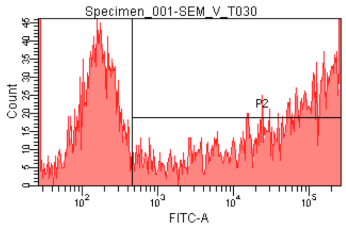

C11.

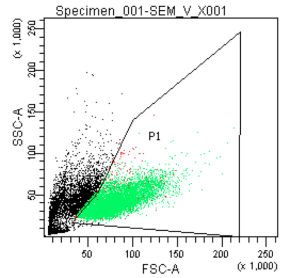

Tube: SEM_V_X001

Population	#Events	%Parent	%Total
All Events	12,211	####	100.0
P1	8,333	68.2	68.2
P2	7,720	92.6	63.2
P3	7,724	92.7	63.3

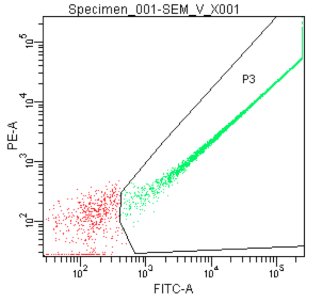

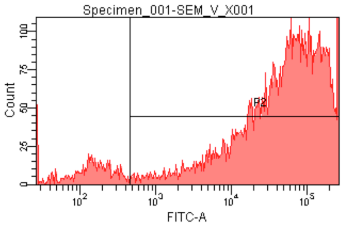

C12.

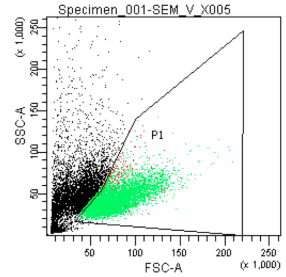

Tube: SEM_V_X005

Population	#Events	%Parent	%Total
All Events	13,499	####	100.0
P1	7,400	54.8	54.8
P2	6,819	92.1	50.5
P3	6,834	92.4	50.6

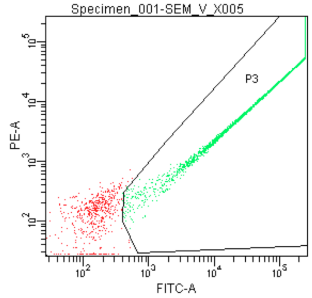

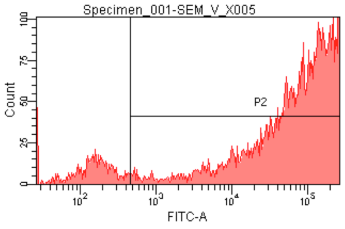

C13.

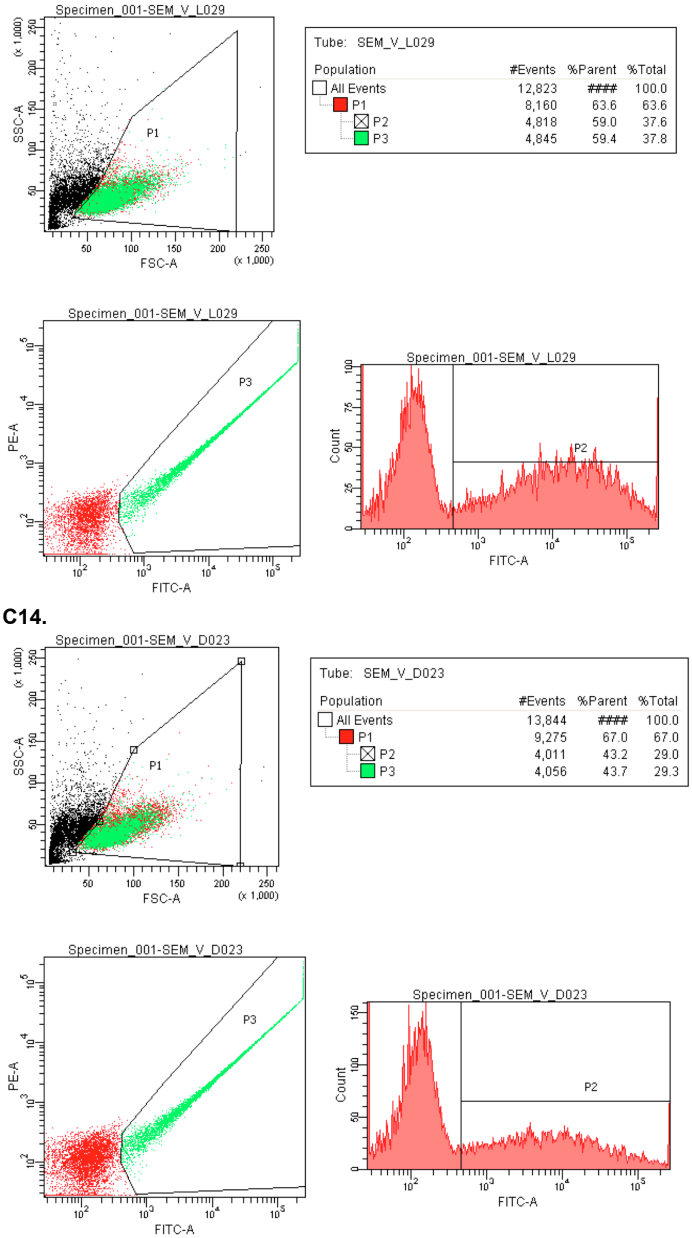

C14.

Figure 4. Amaxa Recommended Optimization protocol for 697, 380 and SEM cell lines.
A1-A7: Solution L, 697. **A8-A14**: Solution V, 697. **B1-B7**: Solution L, 380, **B8-B14**: Solution V, 380. **C1-C7**: Solution L, SEM, **C8-C14**: Solution V, SEM. Optimal protocol for 697 is Solution L Program X001, and for SEM is Solution V Program X001, while no optimal protocol was found for 380.

For the optimization, Nucleofector Solutions L and V were used in 7 different Amaxa nuclefector programs A-020, T-020, X-001, X-005, L-029, and D-023. For each reaction, 1E6 of cells, 100ul of each Nucleofector Solution and 2ug of manufacturer provided GFP plasmid were used. Cells were electroporated and allowed to recover in 1ml of RPMI+15%FBS for 24hrs before being analyzed for fluorescence in LSRII FACS machine (BD BIOSCIENCES).

The optimized protocol for 697 is Nucleofector Solution L, program X-001.

Amaxa nucleofector (LONZABIO, Walkersville MD) was used to electroporate 697 cells with AMBION pre-miRs Negative Control 1 (AM17110), hsa-miR-221 (PM10337), hsa-miR-222 (PM11376). The pre-miRs were used at a quantity of 200 pmole per 1E6 cells, while Program X001 and solution L was used according to manufacturer's instructions. Transfected cells were allowed to incubate at 37ºC, 5% atmosphere for 24hrs before being used for assays.

2.1.8. Plasmid Construction

The Luciferase-Renilla dual-reporter system from Promega (Madison, WI.) was used to assay for the miRNA to 3'UTR association. The luciferase reporter was constructed through the ligation of pGL3-control and PCR amplified Nemo-Like Kinase

3'UTR into the XBaI site. The forward and reverse primers flanking the 3'UTR of Nemo-Like Kinase (NM_016231.4, GI:149408125) were designed on Primer3Plus (http://www.bioinformatics.nl/cgi-bin/primer3plus/primer3plus.cgi). The primer sequences are: NLK_3'UTR_Forward: GCG TCT AGA TG GGA GTG ATG GTG GAA GAT, NLK_3'UTR_Reverse: GCG TCT AGA CAG AAA GTG TGC CAC GGT AA.

2.1.9. Glucocorticoid Sensitivity Assay

Cells were seeded at a density of $1X10^6$ per mL, 200uL per well in 96-well plates. Prednisone is a pro-drug that requires metabolic conversion into its active form Prednisolone, so for the purpose of this study, Prednisolone was used in place of Prednisone. Prednisolone (P6004, SigmaAldrich, St. Louis, MO.) and Dexamethasone (D1756, SigmaAldrich, St. Louis, MO.) were used to determine the sensitivity of the cells to glucocorticoid treatment. The drugs were serially diluted in RPMI to obtain a range of stock concentrations from 4uM to 128uM. 2uL of each drug stock was added to 200uL of cell suspension to obtain final working concentrations of 0.04uM to 1.28uM. 2uL of sterile water was used as negative control. Each treatment was repeated in triplicates. Cells were allowed to incubate for 72hr at 37°C and 5% CO_2 atmosphere before being assayed for viability.

2.1.10. Viability Assay

Cell titre assay (Promega, Madison WI) was used to determine ATP levels, and used according to manufacturer instructions.

2.1.11. Caspase Assay

Caspase-Glo® 3/7 (Promega, Madison WI) was used to determine caspase3/7 levels, and used according to manufacturer instructions.

2.1.12. Proliferation Assay

CellTiter 96® AQueous Non-Radioactive Cell Proliferation Assay (MTS) (Promega, Madison WI) was used to determine formazan levels and used according to manufacturer instructions.

2.1.13. Cell Cycle Analysis

Cells were serum-starved for 24hrs before being used for experiments. After 72hrs treatment and incubation, cells were harvested for analysis. Cells were centrifuged at 2000rpm and aspirated of media, before adding 250uL of PBS, followed by 750uL of 100% ethanol with vortexing and incubation at -20ºC for 15min for fixation. The cells were next centrifuged at 4000rpm and aspirated of the ethanol solution, and 1mL of propidium iodide solution was added to the cells and allowed to incubate at 37ºC for 15min. The cells were analyzed in a LSRII flow cytometer (BD Biosciences, San Diego CA). Every 1mL of propidium iodide

solution was made up of 0.94mL of PBS, 0.05mL of propidium iodide (1.0mg/mL, Sigma), 5uL of RNase A (20mg/mL, Invitrogen, Carlsbad CA), 5uL of Triton X-100 (Diluted to 10% in water, Sigma Aldrich, St Louis MO).

2.1.14. Western Blotting

Cells were harvested and washed with 1X PBS, before being lysed with 1X Cell Lysis Buffer (Cell Signaling Technology, Danvers, MA.). Protein concentrations were quantified with the Bradford Assay before adding equal volumes of Laemmli buffer and denatured at 100ºC for 10min. For each sample, 20ug of cell lysate was loaded onto 4-20% polyacrylamide Tris-HCl Criterion® Gel (BIO-RAD, Hercules, CA.) and run at 80V in a Criterion® midi-format electrophoresis cell. The gel was next transferred onto 0.2um nitrocellulose membrane at 60V for 2hr using Criterion® midi-format Blotter. The transferred membranes were then blocked with blocking buffer made up of 5% BSA dissolved in 1X Tris-Buffered Saline for 1hr at room temperature. After blocking, primary antibodies diluted in 1X incubation buffer made up of 5% BSA dissolved in 1X Tris-Buffered Saline and 0.1% Tween20 were added and incubated overnight at 4ºC with moderate shaking. Following primary antibody incubation, membranes were washed 3X, 5min each time with wash buffer made up of 1X Tris-Buffered Saline and 0.05% Tween20. After washing, the secondary antibody diluted in 1X incubation buffer was added and the

membrane was allowed to incubate at room temperature for 1hr before repeating the washing procedure. 1X TBS was used to rinse off excess detergent before applying the HyGlo (Denville Scientific, Metuchen, NJ.) chemiluminescent horseradish peroxidase detection reagent. Anti-NLK rabbit polyclonal antibody (#AB10206: Millipore, Temecula, CA.) and Anti-GAPDH rabbit monoclonal antibody HRP-conjugate (#3683: Cell Signaling Technology, Danvers, MA.) were used at 5000X dilution in 1X incubation buffer, Anti-Acetyl-CBP rabbit polyclonal antibody (#4771: Cell Signaling Technologies, Danvers, MA.) was used at 1000X dilution, while Anti-Rabbit IgG HRP-conjugate (#7074 Cell Signaling Technology Danvers, MA.) was used at 3000X dilution.

2.1.15. Statistical Testing

Assays were performed in triplicates and Welch's t-test was used to calculate all p-values.

2.2. Results

2.2.1. miRNA Profiling and Screening of Pediatric Normal Karyotype B-cell Precursor ALL Patients

To determine if miRNAs are differentially expressed between ML (n=7) and MH (n=7) patients, an initial miRNA profiling was performed using Low Density Arrays (LDA). The TaqMan Human miRNA Array V2 contains 667 miRNA assays, of which 263

miRNAs were detected in patient samples (Figure 5A-D). After filtering the data with p-value less than 0.05, 50 miRNAs are differentially expressed between ML and MH patients. These 50 miRNAs cluster the patients into 2 distinct groups according to their prognostic response to chemotherapy in hierarchical average linkage (Figure 5E). MH patients have a disproportionate number of miRNAs that are up regulated, i.e. 49 as compared to 1 (miR-509-3p) in ML patients. The fold changes were the greatest for miR221/222 at 7.5 and 6.3 fold respectively in MH patients with respect to ML patients and was calculated as median values of MH expression over median values of ML expression (Figure 6).

A.

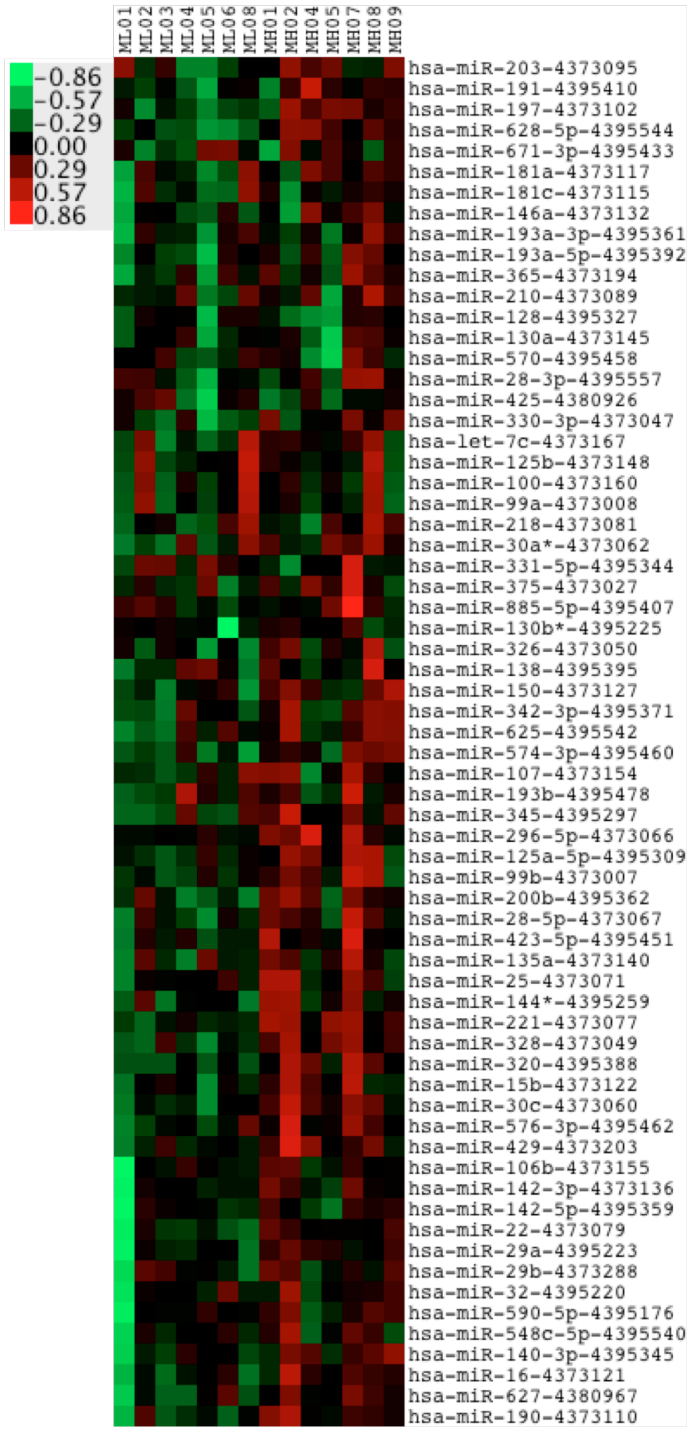
ML01
ML02
ML03
ML04
ML05
ML06
ML08
MH01
MH02
MH04
MH05
MH07
MH08
MH09
-0.86
-0.57
-0.29
0.00
0.29
0.57
0.86
hsa-miR-203-4373095
hsa-miR-191-4395410
hsa-miR-197-4373102
hsa-miR-628-5p-4395544
hsa-miR-671-3p-4395433
hsa-miR-181a-4373117
hsa-miR-181c-4373115
hsa-miR-146a-4373132
hsa-miR-193a-3p-4395361
hsa-miR-193a-5p-4395392
hsa-miR-365-4373194
hsa-miR-210-4373089
hsa-miR-128-4395327
hsa-miR-130a-4373145
hsa-miR-570-4395458
hsa-miR-28-3p-4395557
hsa-miR-425-4380926
hsa-miR-330-3p-4373047
hsa-let-7c-4373167
hsa-miR-125b-4373148
hsa-miR-100-4373160
hsa-miR-99a-4373008
hsa-miR-218-4373081
hsa-miR-30a*-4373062
hsa-miR-331-5p-4395344
hsa-miR-375-4373027
hsa-miR-885-5p-4395407
hsa-miR-130b*-4395225
hsa-miR-326-4373050
hsa-miR-138-4395395
hsa-miR-150-4373127
hsa-miR-342-3p-4395371
hsa-miR-625-4395542
hsa-miR-574-3p-4395460
hsa-miR-107-4373154
hsa-miR-193b-4395478
hsa-miR-345-4395297
hsa-miR-296-5p-4373066
hsa-miR-125a-5p-4395309
hsa-miR-99b-4373007
hsa-miR-200b-4395362
hsa-miR-28-5p-4373067
hsa-miR-423-5p-4395451
hsa-miR-135a-4373140
hsa-miR-25-4373071
hsa-miR-144*-4395259
hsa-miR-221-4373077
hsa-miR-328-4373049
hsa-miR-320-4395388
hsa-miR-15b-4373122
hsa-miR-30c-4373060
hsa-miR-576-3p-4395462
hsa-miR-429-4373203
hsa-miR-106b-4373155
hsa-miR-142-3p-4373136
hsa-miR-142-5p-4395359
hsa-miR-22-4373079
hsa-miR-29a-4395223
hsa-miR-29b-4373288
hsa-miR-32-4395220
hsa-miR-590-5p-4395176
hsa-miR-548c-5p-4395540
hsa-miR-140-3p-4395345
hsa-miR-16-4373121
hsa-miR-627-4380967
hsa-miR-190-4373110

B.

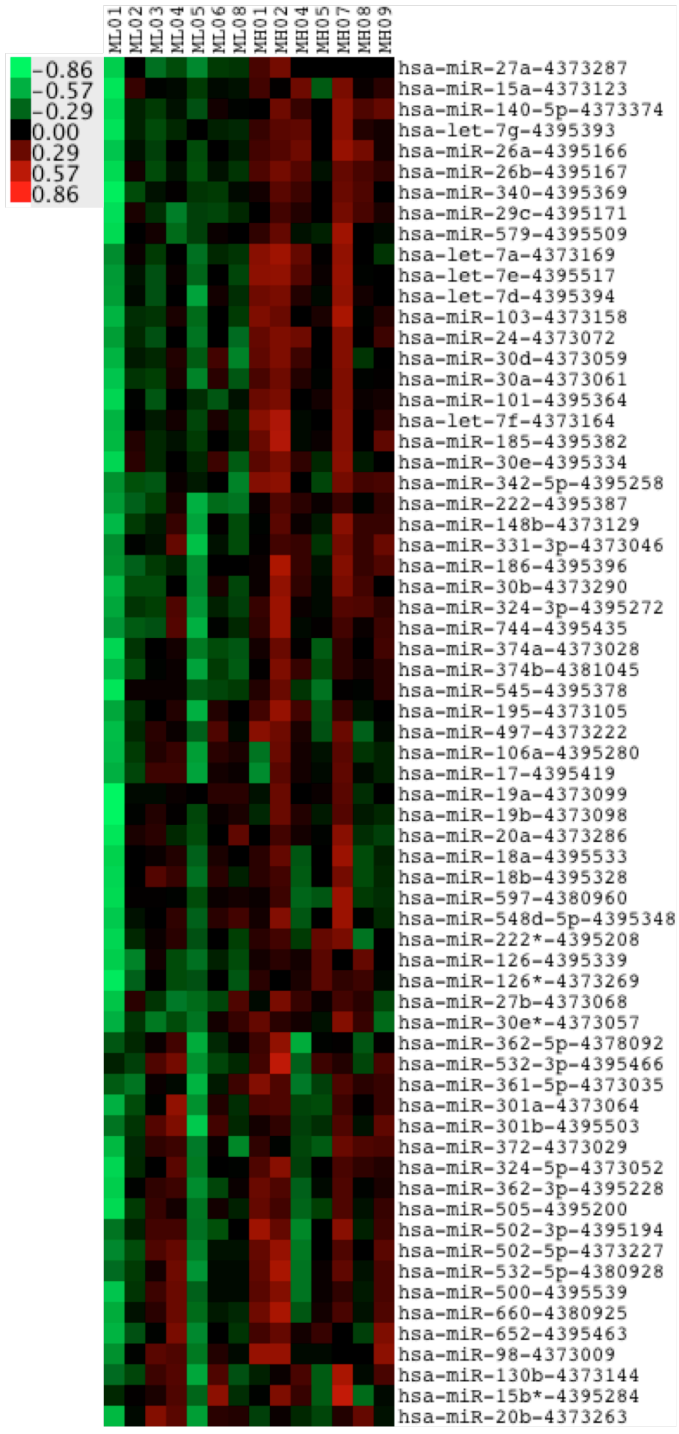
ML01
ML02
ML03
ML04
ML05
ML06
ML08
MH01
MH02
MH04
MH05
MH07
MH08
MH09
-0.86
-0.57
-0.29
0.00
0.29
0.57
0.86
hsa-miR-27a-4373287
hsa-miR-15a-4373123
hsa-miR-140-5p-4373374
hsa-let-7g-4395393
hsa-miR-26a-4395166
hsa-miR-26b-4395167
hsa-miR-340-4395369
hsa-miR-29c-4395171
hsa-miR-579-4395509
hsa-let-7a-4373169
hsa-let-7e-4395517
hsa-let-7d-4395394
hsa-miR-103-4373158
hsa-miR-24-4373072
hsa-miR-30d-4373059
hsa-miR-30a-4373061
hsa-miR-101-4395364
hsa-let-7f-4373164
hsa-miR-185-4395382
hsa-miR-30e-4395334
hsa-miR-342-5p-4395258
hsa-miR-222-4395387
hsa-miR-148b-4373129
hsa-miR-331-3p-4373046
hsa-miR-186-4395396
hsa-miR-30b-4373290
hsa-miR-324-3p-4395272
hsa-miR-744-4395435
hsa-miR-374a-4373028
hsa-miR-374b-4381045
hsa-miR-545-4395378
hsa-miR-195-4373105
hsa-miR-497-4373222
hsa-miR-106a-4395280
hsa-miR-17-4395419
hsa-miR-19a-4373099
hsa-miR-19b-4373098
hsa-miR-20a-4373286
hsa-miR-18a-4395533
hsa-miR-18b-4395328
hsa-miR-597-4380960
hsa-miR-548d-5p-4395348
hsa-miR-222*-4395208
hsa-miR-126-4395339
hsa-miR-126*-4373269
hsa-miR-27b-4373068
hsa-miR-30e*-4373057
hsa-miR-362-5p-4378092
hsa-miR-532-3p-4395466
hsa-miR-361-5p-4373035
hsa-miR-301a-4373064
hsa-miR-301b-4395503
hsa-miR-372-4373029
hsa-miR-324-5p-4373052
hsa-miR-362-3p-4395228
hsa-miR-505-4395200
hsa-miR-502-3p-4395194
hsa-miR-502-5p-4373227
hsa-miR-532-5p-4380928
hsa-miR-500-4395539
hsa-miR-660-4380925
hsa-miR-652-4395463
hsa-miR-98-4373009
hsa-miR-130b-4373144
hsa-miR-15b*-4395284
hsa-miR-20b-4373263

C.

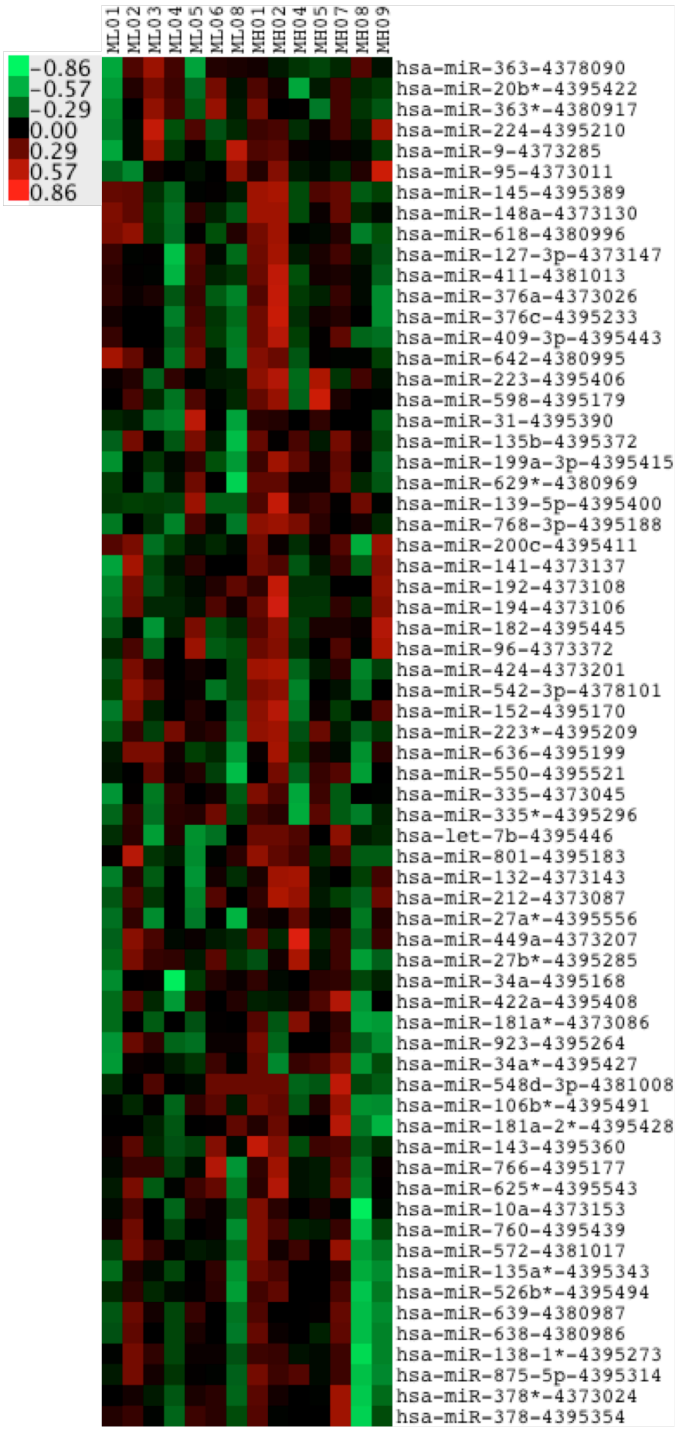
ML01
ML02
ML03
ML04
ML05
ML06
ML08
MH01
MH02
MH04
MH05
MH07
MH08
MH09
-0.86
-0.57
-0.29
0.00
0.29
0.57
0.86
hsa-miR-363-4378090
hsa-miR-20b*-4395422
hsa-miR-363*-4380917
hsa-miR-224-4395210
hsa-miR-9-4373285
hsa-miR-95-4373011
hsa-miR-145-4395389
hsa-miR-148a-4373130
hsa-miR-618-4380996
hsa-miR-127-3p-4373147
hsa-miR-411-4381013
hsa-miR-376a-4373026
hsa-miR-376c-4395233
hsa-miR-409-3p-4395443
hsa-miR-642-4380995
hsa-miR-223-4395406
hsa-miR-598-4395179
hsa-miR-31-4395390
hsa-miR-135b-4395372
hsa-miR-199a-3p-4395415
hsa-miR-629*-4380969
hsa-miR-139-5p-4395400
hsa-miR-768-3p-4395188
hsa-miR-200c-4395411
hsa-miR-141-4373137
hsa-miR-192-4373108
hsa-miR-194-4373106
hsa-miR-182-4395445
hsa-miR-96-4373372
hsa-miR-424-4373201
hsa-miR-542-3p-4378101
hsa-miR-152-4395170
hsa-miR-223*-4395209
hsa-miR-636-4395199
hsa-miR-550-4395521
hsa-miR-335-4373045
hsa-miR-335*-4395296
hsa-let-7b-4395446
hsa-miR-801-4395183
hsa-miR-132-4373143
hsa-miR-212-4373087
hsa-miR-27a*-4395556
hsa-miR-449a-4373207
hsa-miR-27b*-4395285
hsa-miR-34a-4395168
hsa-miR-422a-4395408
hsa-miR-181a*-4373086
hsa-miR-923-4395264
hsa-miR-34a*-4395427
hsa-miR-548d-3p-4381008
hsa-miR-106b*-4395491
hsa-miR-181a-2*-4395428
hsa-miR-143-4395360
hsa-miR-766-4395177
hsa-miR-625*-4395543
hsa-miR-10a-4373153
hsa-miR-760-4395439
hsa-miR-572-4381017
hsa-miR-135a*-4395343
hsa-miR-526b*-4395494
hsa-miR-639-4380987
hsa-miR-638-4380986
hsa-miR-138-1*-4395273
hsa-miR-875-5p-4395314
hsa-miR-378*-4373024
hsa-miR-378-4395354

D.

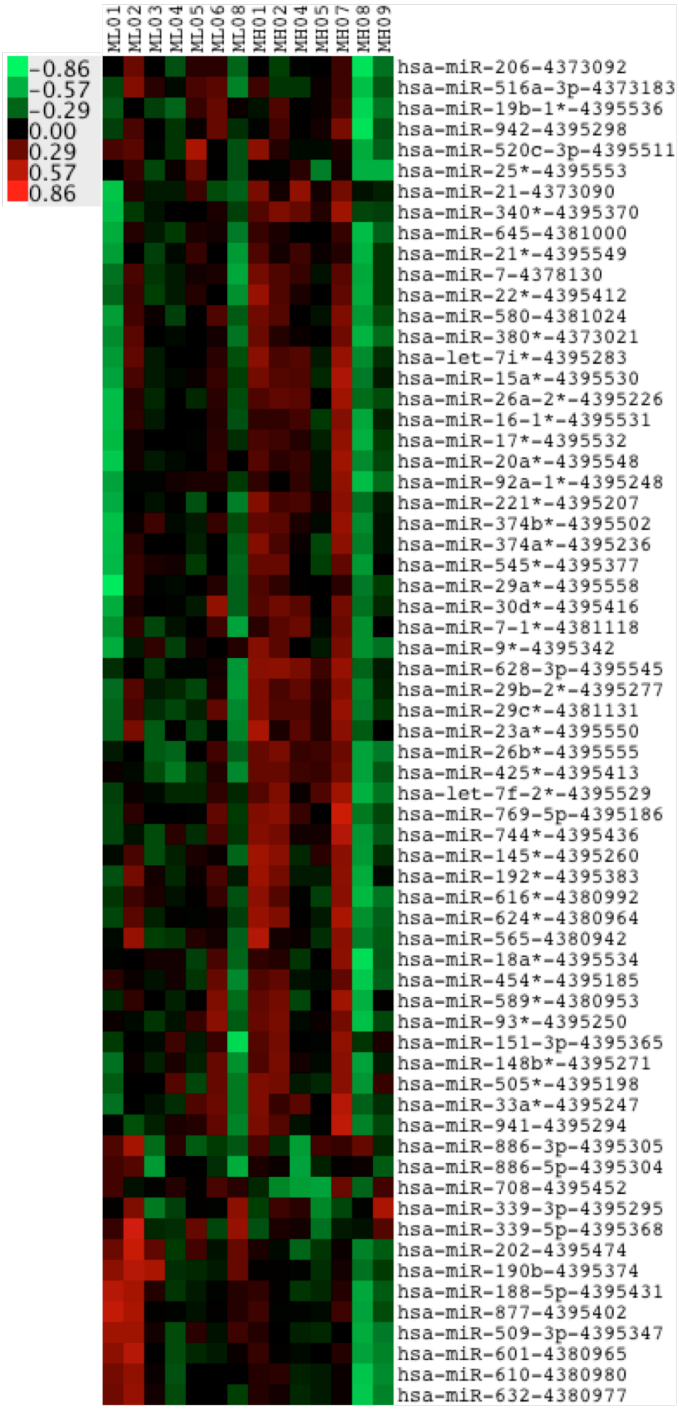
ML01
ML02
ML03
ML04
ML05
ML06
ML08
MH01
MH02
MH04
MH05
MH07
MH08
MH09
-0.86
-0.57
-0.29
0.00
0.29
0.57
0.86
hsa-miR-206-4373092
hsa-miR-516a-3p-4373183
hsa-miR-19b-1*-4395536
hsa-miR-942-4395298
hsa-miR-520c-3p-4395511
hsa-miR-25*-4395553
hsa-miR-21-4373090
hsa-miR-340*-4395370
hsa-miR-645-4381000
hsa-miR-21*-4395549
hsa-miR-7-4378130
hsa-miR-22*-4395412
hsa-miR-580-4381024
hsa-miR-380*-4373021
hsa-let-7i*-4395283
hsa-miR-15a*-4395530
hsa-miR-26a-2*-4395226
hsa-miR-16-1*-4395531
hsa-miR-17*-4395532
hsa-miR-20a*-4395548
hsa-miR-92a-1*-4395248
hsa-miR-221*-4395207
hsa-miR-374b*-4395502
hsa-miR-374a*-4395236
hsa-miR-545*-4395377
hsa-miR-29a*-4395558
hsa-miR-30d*-4395416
hsa-miR-7-1*-4381118
hsa-miR-9*-4395342
hsa-miR-628-3p-4395545
hsa-miR-29b-2*-4395277
hsa-miR-29c*-4381131
hsa-miR-23a*-4395550
hsa-miR-26b*-4395555
hsa-miR-425*-4395413
hsa-let-7f-2*-4395529
hsa-miR-769-5p-4395186
hsa-miR-744*-4395436
hsa-miR-145*-4395260
hsa-miR-192*-4395383
hsa-miR-616*-4380992
hsa-miR-624*-4380964
hsa-miR-565-4380942
hsa-miR-18a*-4395534
hsa-miR-454*-4395185
hsa-miR-589*-4380953
hsa-miR-93*-4395250
hsa-miR-151-3p-4395365
hsa-miR-148b*-4395271
hsa-miR-505*-4395198
hsa-miR-33a*-4395247
hsa-miR-941-4395294
hsa-miR-886-3p-4395305
hsa-miR-886-5p-4395304
hsa-miR-708-4395452
hsa-miR-339-3p-4395295
hsa-miR-339-5p-4395368
hsa-miR-202-4395474
hsa-miR-190b-4395374
hsa-miR-188-5p-4395431
hsa-miR-877-4395402
hsa-miR-509-3p-4395347
hsa-miR-601-4380965
hsa-miR-610-4380980
hsa-miR-632-4380977

E.

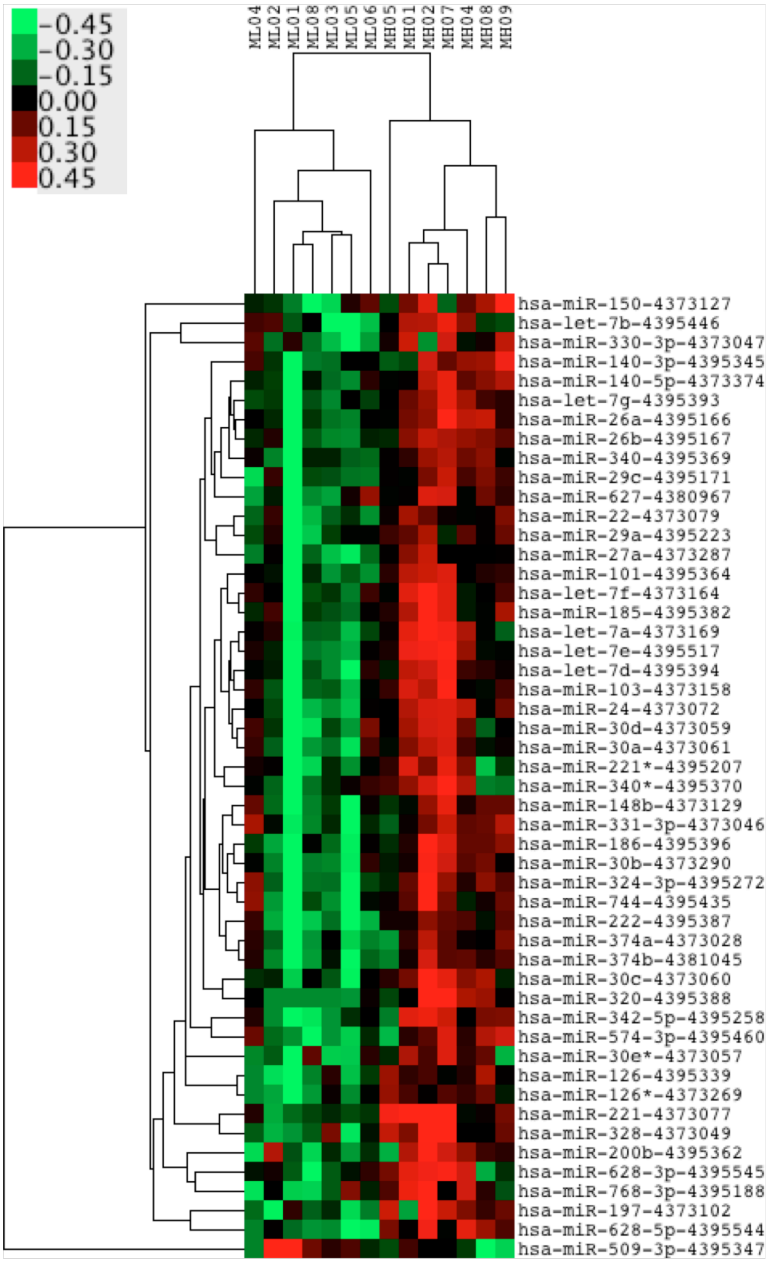

Figure 5. Heatmaps of miRNAs expressed in normal karyotype B-cell precursor ML and MH patients. Auto baseline and auto threshold were used to determine Ct values. All Ct values were normalized to RNU48. Using Gene Cluster 3.0, values were log transformed, centered on the median value across patient samples and normalized before hierarchical average clustering. **A-D**. Heatmap of 263 miRNA expressed in all patient samples and miRNAs clustered by average linkage. **E**. Heatmap of 50 miRNAs filtered by pvalue less than 0.05, miRNAs and patients clustered by hierarchical average linkage.

No.	Detector	ML01	ML02	ML03	ML04	ML05	ML06	ML08	MH01	MH02	MH04	MH05	MH07	MH08	MH09	Median ML	Median MH	Fold Change	p-value
1	hsa-let-7a-4373169	0.00996	0.03478	0.02067	0.03185	0.01330	0.02358	0.02099	0.08148	0.10282	0.06181	0.03259	0.09016	0.02942	0.02113	0.02099	0.06181	2.9	0.0218
2	hsa-let-7b-4395446	0.01182	0.02785	0.00310	0.02666	0.00366	0.00561	0.01958	0.05304	0.05482	0.04085	0.01841	0.08040	0.01411	0.01288	0.01182	0.04085	3.5	0.0422
3	hsa-let-7d-4395394	0.01002	0.02904	0.01893	0.03091	0.00984	0.03626	0.02423	0.06535	0.07151	0.03901	0.02929	0.08598	0.03643	0.03334	0.02423	0.03901	1.6	0.0137
4	hsa-let-7e-4395517	0.03609	0.12936	0.07801	0.16967	0.06339	0.15633	0.08480	0.50647	0.52571	0.29861	0.17122	0.55297	0.14084	0.14661	0.08480	0.29861	3.5	0.0169
5	hsa-let-7f-4373164	0.00129	0.00595	0.00495	0.00709	0.00359	0.00747	0.00448	0.01628	0.02388	0.00543	0.00586	0.01611	0.00617	0.00787	0.00495	0.00787	1.6	0.0495
6	hsa-let-7g-4395393	0.00877	0.05019	0.03568	0.04691	0.06123	0.04877	0.04600	0.09067	0.11300	0.12063	0.06343	0.17040	0.07827	0.07113	0.04691	0.09067	1.9	0.0048
7	hsa-miR-101-4395364	0.00015	0.00160	0.00077	0.00175	0.00111	0.00077	0.00142	0.00488	0.00559	0.00177	0.00210	0.00617	0.00209	0.00221	0.00111	0.00221	2.0	0.0137
8	hsa-miR-103-4373158	0.00241	0.00791	0.00768	0.01306	0.00485	0.01053	0.00734	0.02763	0.02298	0.01140	0.01332	0.04031	0.01032	0.01400	0.00768	0.01400	1.8	0.0251
9	hsa-miR-126-4395339	0.00855	0.03357	0.27845	0.07699	0.04590	0.14228	0.07979	0.29131	0.33902	0.27120	0.65986	0.20355	0.75189	0.22431	0.07699	0.29131	3.8	0.0111
10	hsa-miR-140-3p-4395345	0.00037	0.00091	0.00078	0.00118	0.00102	0.00101	0.00076	0.00087	0.00170	0.00143	0.00083	0.00126	0.00146	0.00189	0.00091	0.00143	1.6	0.0213
11	hsa-miR-140-5p-4373374	0.00954	0.02905	0.02533	0.03100	0.02276	0.03772	0.03229	0.03458	0.05742	0.04310	0.03338	0.06754	0.04859	0.05533	0.02905	0.04859	1.7	0.0034
12	hsa-miR-148b-4373129	0.00026	0.00052	0.00059	0.00083	0.00030	0.00069	0.00048	0.00064	0.00096	0.00071	0.00059	0.00123	0.00083	0.00083	0.00052	0.00083	1.6	0.0199
13	hsa-miR-150-4373127	0.88203	1.16925	0.58020	1.23952	1.55137	1.86845	0.47346	2.02925	3.25613	1.89804	1.06922	0.98103	2.55588	4.61594	1.16925	2.02925	1.7	0.0456
14	hsa-miR-185-4395382	0.00050	0.00269	0.00162	0.00190	0.00143	0.00225	0.00175	0.00438	0.00825	0.00197	0.00244	0.00546	0.00209	0.00416	0.00175	0.00416	2.4	0.0318
15	hsa-miR-186-4395396	0.01371	0.01977	0.02547	0.03025	0.01416	0.03722	0.03579	0.04041	0.11195	0.04977	0.03168	0.08162	0.04945	0.05727	0.02547	0.04977	2.0	0.0144
16	hsa-miR-197-4373102	0.00778	0.00338	0.00631	0.00535	0.00367	0.00503	0.00554	0.00448	0.01482	0.00961	0.01220	0.01211	0.00796	0.00897	0.00535	0.00961	1.8	0.0091
17	hsa-miR-200b-4395362	0.00017	0.00031	0.00019	0.00012	0.00014	0.00019	0.00012	0.00032	0.00040	0.00029	0.00013	0.00035	0.00023	0.00022	0.00017	0.00029	1.7	0.0357
18	hsa-miR-22-4373079	0.00001	0.00064	0.00024	0.00022	0.00034	0.00016	0.00011	0.00146	0.00088	0.00043	0.00051	0.00051	0.00049	0.00107	0.00022	0.00051	2.3	0.0124
19	**hsa-miR-221-4373077**	**0.00369**	**0.00225**	**0.00538**	**0.00834**	**0.00450**	**0.00514**	**0.00457**	**0.04363**	**0.03821**	**0.00628**	**0.03436**	**0.04025**	**0.00747**	**0.01309**	**0.00457**	**0.03436**	**7.5**	**0.0139**
20	**hsa-miR-222-4395387**	**0.17931**	**0.42532**	**0.69619**	**2.08638**	**0.11752**	**0.38117**	**0.32085**	**1.73403**	**3.82425**	**2.42506**	**1.71668**	**2.73811**	**1.30409**	**2.54509**	**0.38117**	**2.42506**	**6.4**	**0.0013**
21	hsa-miR-24-4373072	0.03987	0.10350	0.07551	0.13447	0.05802	0.13690	0.06189	0.26279	0.32011	0.27806	0.13280	0.32755	0.13008	0.19523	0.07551	0.26279	3.5	0.0024
22	hsa-miR-26a-4395166	0.01756	0.11224	0.07604	0.13405	0.06907	0.13193	0.10478	0.22314	0.26374	0.34111	0.12754	0.51813	0.36372	0.15604	0.10478	0.26374	2.5	0.0084
23	hsa-miR-26b-4395167	0.00810	0.06934	0.03380	0.05212	0.03305	0.05264	0.04149	0.10530	0.14314	0.11111	0.05150	0.12706	0.10156	0.08479	0.04149	0.10530	2.5	0.0008
24	hsa-miR-27a-4373287	0.00167	0.00801	0.00366	0.00495	0.00303	0.00540	0.00558	0.01230	0.01647	0.00796	0.00806	0.00790	0.00779	0.00807	0.00495	0.00806	1.6	0.0060
25	hsa-miR-29a-4395223	0.00682	0.05557	0.04034	0.03862	0.04841	0.04809	0.02184	0.06792	0.09411	0.06752	0.06090	0.04326	0.05135	0.07093	0.04034	0.06752	1.7	0.0084
26	hsa-miR-29c-4395171	0.00175	0.01262	0.00786	0.00420	0.00683	0.00673	0.00806	0.01033	0.01607	0.01331	0.01078	0.02288	0.01642	0.01277	0.00683	0.01331	1.9	0.0030
27	hsa-miR-30b-4373290	0.08554	0.21008	0.20698	0.33652	0.12658	0.40832	0.21566	0.37325	0.95944	0.46994	0.31616	0.78314	0.51986	0.35645	0.21008	0.46994	2.2	0.0137
28	hsa-miR-30c-4373060	0.10859	0.20912	0.17781	0.19944	0.09313	0.22883	0.23126	0.32449	0.79499	0.35016	0.25767	0.50855	0.40429	0.20653	0.19944	0.35016	1.8	0.0216
29	hsa-miR-320-4395388	0.02694	0.02674	0.02675	0.04646	0.02597	0.04760	0.02667	0.04513	0.15538	0.08592	0.03636	0.17005	0.08007	0.04683	0.02675	0.08007	3.0	0.0334
30	hsa-miR-324-3p-4395272	0.00076	0.00177	0.00167	0.00380	0.00089	0.00195	0.00164	0.00328	0.00646	0.00268	0.00218	0.00393	0.00383	0.00311	0.00167	0.00328	2.0	0.0152
31	hsa-miR-328-4373049	0.00354	0.00310	0.00937	0.00458	0.00239	0.00578	0.00460	0.00960	0.01951	0.00627	0.01303	0.01743	0.00623	0.00889	0.00458	0.00960	2.1	0.0137
32	hsa-miR-330-3p-4373047	0.00017	0.00010	0.00007	0.00020	0.00003	0.00008	0.00010	0.00033	0.00008	0.00014	0.00016	0.00034	0.00016	0.00030	0.00010	0.00016	1.6	0.0366
33	hsa-miR-331-3p-4373046	0.02140	0.05068	0.04655	0.09351	0.01338	0.04693	0.03345	0.05527	0.07648	0.07068	0.03893	0.10499	0.07251	0.09741	0.04655	0.07251	1.6	0.0406
34	hsa-miR-340-4395369	0.00016	0.00316	0.00666	0.00969	0.00427	0.00399	0.00691	0.01151	0.02659	0.01856	0.00911	0.03410	0.02336	0.00809	0.00427	0.01856	4.4	0.0090
35	hsa-miR-342-5p-4395258	0.00022	0.00039	0.00037	0.00079	0.00058	0.00069	0.00024	0.00186	0.00197	0.00071	0.00041	0.00165	0.00110	0.00114	0.00039	0.00114	2.9	0.0109
36	hsa-miR-374a-4373028	0.01007	0.06666	0.10818	0.12947	0.03290	0.05549	0.04792	0.13280	0.28170	0.11627	0.04668	0.16362	0.10784	0.19553	0.05549	0.13280	2.4	0.0267
37	hsa-miR-374b-4381045	0.01404	0.04118	0.06926	0.08521	0.01801	0.04875	0.03612	0.08079	0.19869	0.10914	0.04151	0.10497	0.08811	0.10272	0.04118	0.10272	2.5	0.0178
38	hsa-miR-574-3p-4395460	0.00236	0.00305	0.00231	0.00836	0.00156	0.00430	0.00100	0.00617	0.00771	0.00620	0.00181	0.01705	0.01296	0.01574	0.00236	0.00771	3.3	0.0250
39	hsa-miR-627-4380967	0.00000	0.00001	0.00001	0.00001	0.00002	0.00002	0.00001	0.00001	0.00003	0.00001	0.00001	0.00003	0.00002	0.00002	0.00001	0.00002	2.0	0.0446
40	hsa-miR-628-5p-4395544	0.00024	0.00036	0.00021	0.00022	0.00012	0.00013	0.00020	0.00036	0.00090	0.00086	0.00052	0.00034	0.00061	0.00045	0.00021	0.00052	2.5	0.0042
41	hsa-miR-744-4395435	0.00312	0.00478	0.00496	0.01220	0.00262	0.00757	0.00639	0.01002	0.01913	0.00720	0.00822	0.01102	0.00842	0.01059	0.00496	0.01002	2.0	0.0328
42	hsa-miR-30d-4373059	0.30165	0.35250	0.34951	0.37068	0.33353	0.38127	0.31902	0.39041	0.40155	0.37816	0.36147	0.40373	0.34548	0.36032	0.34951	0.37816	1.1	0.0314
43	hsa-miR-628-3p-4395545	0.21582	0.22726	0.21554	0.22317	0.22326	0.22985	0.19399	0.25523	0.25679	0.25163	0.23756	0.25880	0.20495	0.22028	0.22317	0.25163	1.1	0.0352
44	hsa-miR-768-3p-4395188	0.37126	0.39046	0.38351	0.36907	0.40206	0.38832	0.37097	0.41395	0.41657	0.41018	0.39682	0.39138	0.39388	0.38446	0.38351	0.39682	1.0	0.0151
45	hsa-miR-126*-4373269	0.28046	0.34799	0.39454	0.35696	0.35545	0.38808	0.35236	0.40645	0.39272	0.40271	0.42917	0.40967	0.41525	0.38361	0.35545	0.40645	1.1	0.0090
46	hsa-miR-221*-4395207	0.18033	0.23826	0.23054	0.24048	0.21131	0.23563	0.19682	0.28411	0.25900	0.25989	0.24430	0.28719	0.20113	0.22810	0.23054	0.25900	1.1	0.0444
47	hsa-miR-30a-4373061	0.34699	0.39506	0.39193	0.41738	0.37001	0.42019	0.38449	0.43030	0.44256	0.41954	0.40717	0.44847	0.40649	0.41224	0.39193	0.41954	1.1	0.0139
48	hsa-miR-30e*-4373057	0.32853	0.35656	0.34159	0.35102	0.34235	0.36993	0.37570	0.38562	0.37324	0.37066	0.36199	0.39291	0.37629	0.34507	0.35102	0.37324	1.1	0.0389
49	hsa-miR-340*-4395370	0.25444	0.29145	0.30028	0.30400	0.30695	0.31192	0.28943	0.32629	0.33970	0.33183	0.31451	0.35140	0.28801	0.28970	0.30028	0.32629	1.1	0.0463
50	hsa-miR-509-3p-4395347	0.29772	0.29582	0.23425	0.20182	0.24147	0.21989	0.24855	0.23960	0.22734	0.21608	0.21355	0.22664	0.16647	0.18401	0.24147	0.21608	0.9	0.0463

Figure 6 Low Density Array qRT-PCR profiling data of 7ML and 7MH. Fold change is measured as median ML over median MH expression values. These 50 miRNAs are expressed in all samples and have been filtered at p values less than 0.05 using Welch's t-test.

2.2.2. Validation of let-7e, miR-24, miR-29a, miR-30b, miR-221 and miR-222 in Enlarged Pool of Pediatric Normal Karyotype ALL Patients

The following miRNAs were selected for TaqMan miRNA Assay in an enlarged pool of 18 ML and 15 MH patients: let-7e, miR-24, miR-29a, miR-30b, miR-221 and miR-222. The LDA data was validated for miR-24, miR-29a, miR-30b, miR-221 and miR-222 in which the over expression of miRNAs in MH patients compared to ML patients were significant at pvalues less than 0.05, while the expression of let-7e was not significantly different (Figure 7).

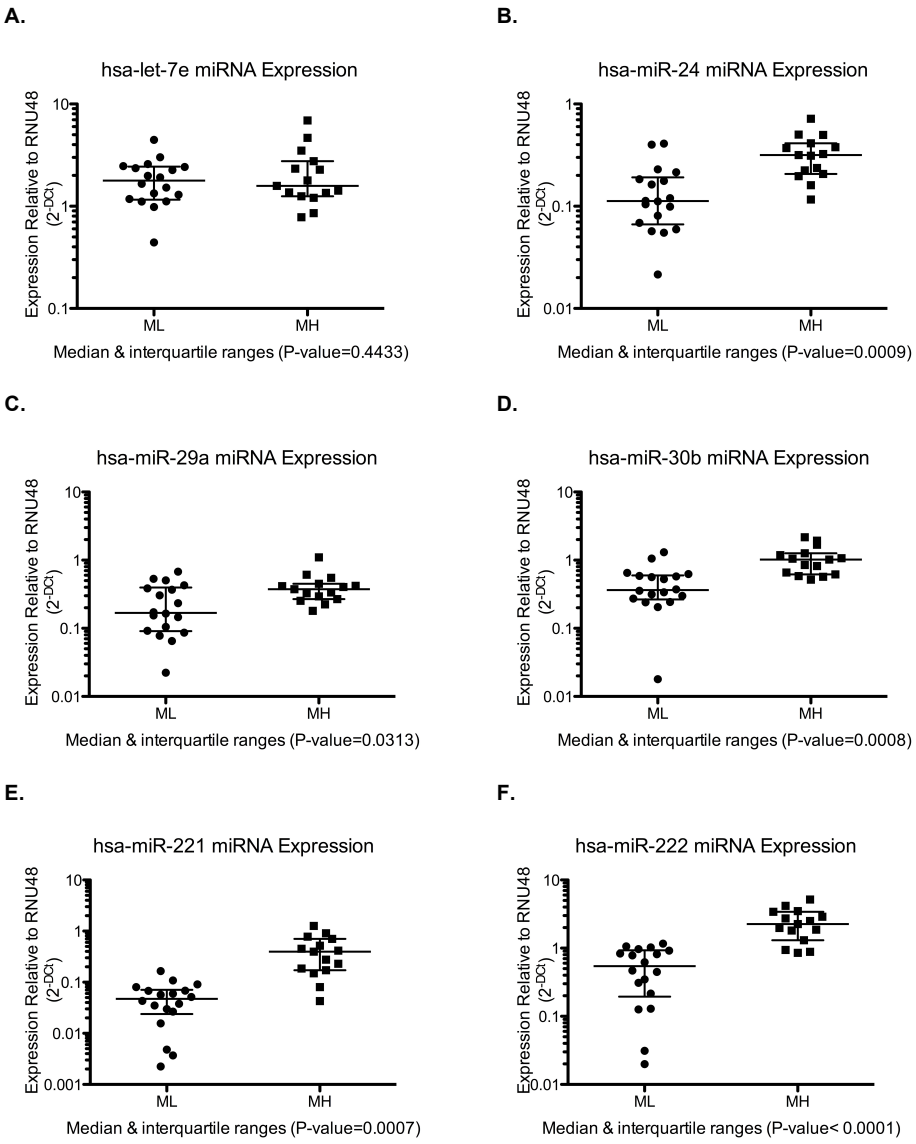

Figure 7. Gene Expression assays to validate differential expression of miRNAs in ML and MH patients. Dot plots show that miR-24, miR-29a, miR-30b, miR-221 and miR-222 are up regulated in MH over ML patients with mean levels of 2.2, 1.65, 2.2, 8.3 and 4.2 fold respectively with p values less than 0.05 calculated by Welch's t-test, while let-7e expression was not significantly different.

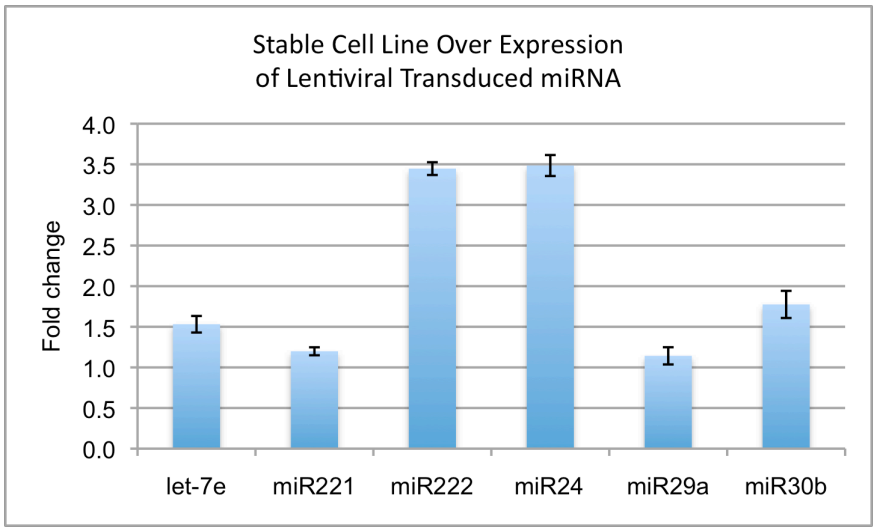

Figure 8. Fold changes indicating levels of over expression achieved by lentiviral delivery of miRNA pre-miR constructs into 697 cell line. Fold changes are relative to 697 transduced with the pCDH-MSCV-MCS-EF1-GFP-PURO empty vector and normalized to RNU48.

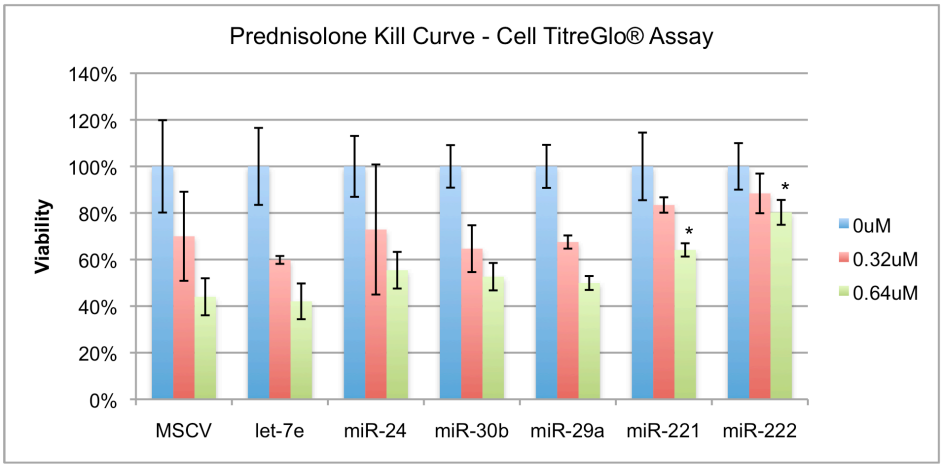

Figure 9. Screening 697 cell stable cell lines that over express select miRNAs for resistance to glucocorticoids. Asterisks indicate data points with values significant at pvalues less than 0.05, calculated using Welch's t-test. At 0.64uM, for 697 stable cell line over expressing miR-221 and miR-222, the pvalues are 0.0287 and 0.0026 respectively.

Stable cell lines over expressing let-7e, miR-24, miR-29a, miR-30b, miR-221 and miR-222 were constructed to analyze their ability in mediating resistance to glucocorticoids. Over expression of miRNA in each stable cell line were validated by qRT-PCR (Figure 8).

In treatments with Prednisolone, cell lines over expressing miR-221 and miR-222 showed the most resistance (Figure 9), and were selected for further experiments to ascertain the mechanism of resistance.

2.2.3. miR221/222 Over-expression Modulates Prednisolone Activity in B-cell Precursor ALL

Based on the LDA qRT-PCR and Prednisolone screening data, high levels of miR-221/222 might mediate chemotherapy resistance and predispose patients to relapse. Since steroids are one of the cornerstones of ALL therapeutics, it was investigated whether miR-221/222 mediate steroid resistance. In order to demonstrate this hypothesis, stable 697 cell lines over expressing miR-221/222 were assayed for apoptosis, viability, proliferation and cell cycle activity after Prednisolone treatment.

At the maximum Prednisolone concentration of 0.64uM, cell lines over expressing miR-221/222 showed reduced sensitivity to Prednisolone (64% and 80%), reduced apoptotic activity (6.8 and 6.1-fold) and increased proliferative activity (45% and 55%) when compared to the cell line over-expressing the empty lentivector

(44%, 7.1-fold, 41%) (Figure 10). And when combined with cell cycle analysis data of miR-221/222 over expressing cells showing approximately 20% increase in S phase cells, it indicates a possible correlation miR-221/222 with reduced Prednisolone sensitivity through S-phase cell cycle arrest.

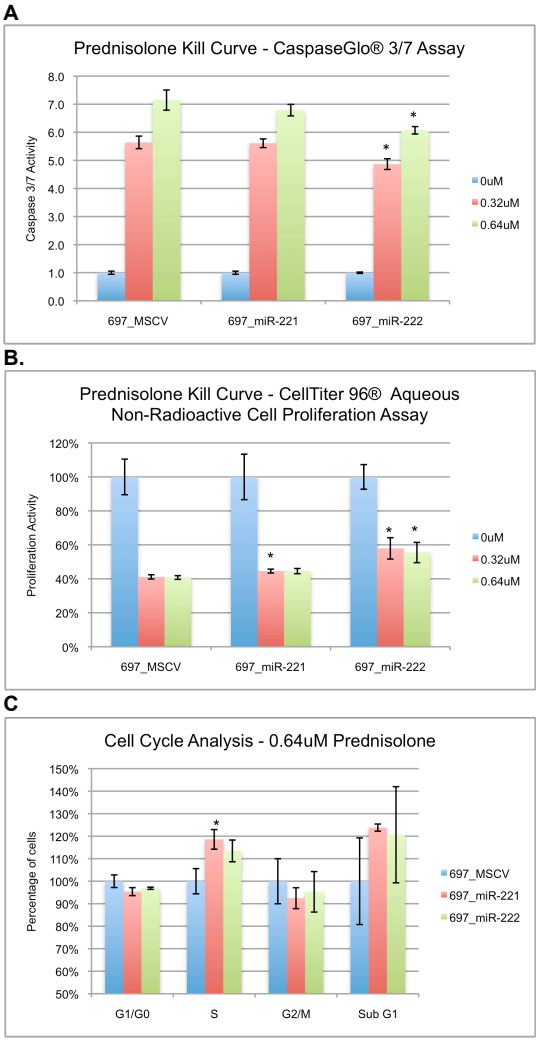

Figure 10. Assays used to determine the general process of resistance mediated by miR-221/222. Cell lines over-expressing miR-221/222 generally show lower caspase activity, greater proliferation and an increase of cells in S phase over the cell line over expressing the empty vector. Error bars indicate standard deviation of 3 replicates. Data significant at pvalue of less than 0.05, calculated using Welch's t-test are marked with an asterisk.

2.2.4. Target Identification: Proteins Modulated by miR-221/222

Based on the information that over expression of miR-221/222

reduces sensitivity of B-cell precursor 697 cell line to Prednisolone, and that miRNAs function to down regulate cellular protein levels, the goal was to identify a tumor suppressor. Literature on tumor suppressors was reviewed to identify potential target candidates of miR-221/222, and cross-referencing with TargetScan database identified Nemo-Like Kinase (NLK) as a candidate gene.

NLK was previously reported to induce apoptosis in solid tumors like glioma[28], prostate[29] and colon[30] cancer as well as regulating a broad range of transcription factors[31], in addition to TargetScan database providing a strong seed sequence match prediction of 7mer-m8 (Figure 12A). Since the tumor suppressive effects of NLK was only reported in solid tumors, it would be a novel discovery if the same results could also be identified in leukemia.

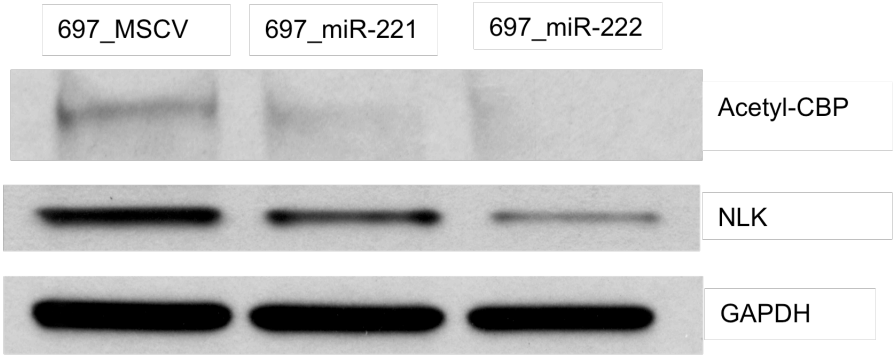

Figure 11. Analysis of miR-221/222 over expression on relative abundance of endogeneous protein levels. Western blotting shows the reduction of NLK in tandem with acetylated CBP in cell lines over expressing miR-221 and miR-222.

In western-blotting of 697 stable cell lines over expressing the empty lentivector and miR-221/222 and normalizing with GAPDH, it was observed that NLK protein levels were reduced with miR-

221/222 over expression. The direct interaction of NLK with miR-221/222 was confirmed through luciferase reporter assays of NLK 3'UTR with miR-221/222 (Figure 12B).

A.

Position 32-38 of NLK 3' UTR	**Predicted consequential pairing of target region (top) and miRNA (bottom)**
miR-221	5' ...ACUACUGAAGAUGUAAUGUAGCU... ||||||| 3' CUUUGGGUCGUCUGUUACAUCGA
miR-222	5' ...ACUACUGAAGAUGUAAUGUAGCU... ||||||| 3' UGGGUCAUCGGUCUACAUCGA

B.

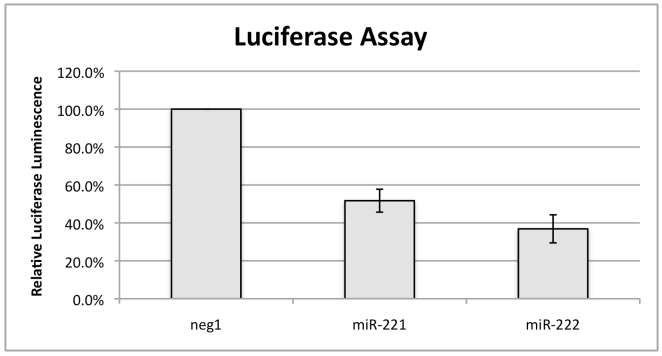

Figure 12. Validation of NLK as target of miR221/222. (A) From TARGETSCAN registry, miR-221/222 were identified to have seed sequences complementary to the 3'UTR of NLK mRNA. (B). Luciferase assay confirmed the interaction of miR-221/222 with 3'UTR of NLK mRNA, resulting in greater than 50% reduction in luciferase activity, due to seed sequence complementary binding and subsequent translation inhibition. The p-values for miR-221 and miR-222 are 0.0033 and 0.0035 respectively calculated using Welch's t-test.

2.2.5. Validation of NLK expression in B-cell Precursor ALL Patients

The NLK mRNA expression in the ML and MH patients were validated using Taqman Gene Expression Assays by qRT-PCR. The median level of NLK mRNA was approximately 3-fold higher in the ML than MH patients (Figure 13).

A.

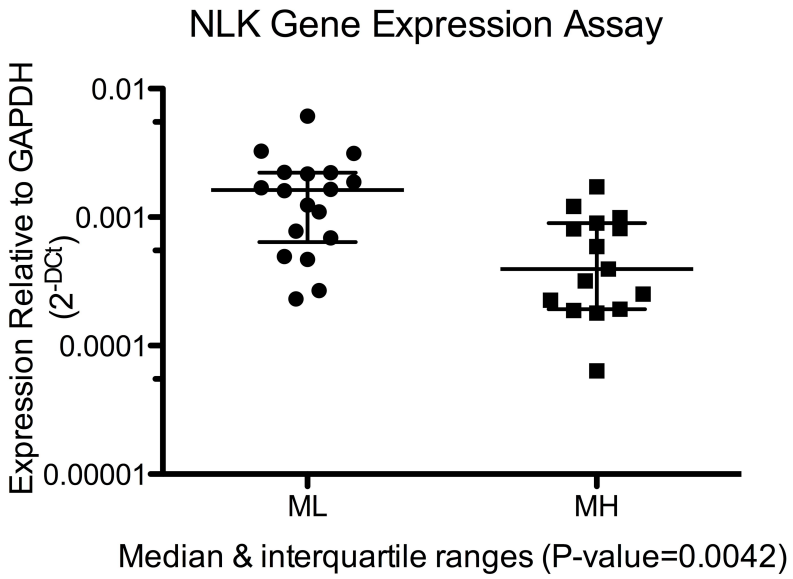

Figure 13 Gene expression assays to determine levels of expression between ML and MH patients. NLK (A) median expressions are approximately 3-fold higher in ML than MH patients. NR3C1 (B) and CBP (C) median expressions showed no significant difference. Welch's t-test was used to calculate pvalues.

2.3. Discussion

In comparing the miRNA expression profile between ML(n=7) and MH(n=7) patients with normal karyotypes, a group of 49 miRNAs were significantly (pvalue<0.05) upregulated in the MH patients. Hierarchical average clustering analysis was in concordance with patients' MRD response to chemotherapy. From this group of miRNAs, miR-221 and miR-222 were chosen for Single Assay validation in an enlarged pool of ML(n=18) and MH(n=15) patients, in which both miRNAs shown to be upregulated in MH patients at pvalues less than 0.05. These 2 miRNAs were chosen for further analysis as they exhibit the greatest fold change in MH over ML patients and had been implicated in resistance[24] and oncogenesis[25,26,27] mechanisms in previous studies, hence are the most probable contributors to chemotherapy resistance of this study.

Stable cell lines over expressing miR-221/222 were constructed using pre-B cell line 697, to assess the miRNAs' functionalities in affording resistance to the glucocorticoid Prednisolone. After treatment with Prednisolone, cell lines over-expressing miR-221/222 were observed to have decreased sensitivity to Prednisolone in the form of higher viability, lower caspase activity and increased proliferation over the negative control. Cell cycle analysis correlates with the sensitivity data in which there is an approximately 20% increase in S phase for cells over expressing

miR-221/222 as compared to the control cells. These results indicate a partial cell cycle arrest at S phase (Figure 10C).

The summation of the assay results suggest that proliferation advantage and reduced apoptotic activity contributes to miR-221/222 mediated glucocorticoid resistance. So it is probable that excessive leukemic clones are generated by dys-regulated mitosis and impaired apoptosis mechanisms increase the survival of leukemic clones in the presence of cytotoxic pressure.

Hence, the protein target of miR-221/222 should be a tumor suppressor and was identified through literature search and cross-referencing with TargetScan database. The candidate protein was narrowed down to NLK, and western blotting results showed reduced levels of NLK in miR-221/222 over expressed cell lines and confirmed through luciferase assays which determined that luciferase activity was reduced by greater than 50% when miR-221 and miR-222 were used in the assays.

The expression of NLK mRNA was also validated in patient samples through qRT-PCR. The results showed that NLK mRNA was significantly expressed in ML patients compared to MH patients by 3-fold, at pvalue of less than 0.05. This result underscores the biological significance of NLK in differentiating Normal Karyotype patients with heterogeneous responses to glucocorticoid treatment. Furthermore this result is significant as

previously, implications of NLK in the control of carcinogenesis were only reported in solid tumors and this study is the first instance of correlating NLK with chemoresistance in leukemia.

Chapter 3: Summary, Conclusions and Future Perspectives

3.1. Current Understanding of NK B-cell Precursor ALL

By excluding the most frequent and prognostically relevant chromosomal abnormalities, 20-25% of pediatric ALL patients are considered as without a prognostic genetic indicator. The definition of 'normal karyotype' is herewith operational, depending on the type and sensitivity of the diagnostic method applied. Those patients exhibit heterogeneous response to glucocorticoid-based chemotherapy as well as variable relapse rates.

Currently there is no specific treatment to improve on normal karyotype survival rates, as there is minimal information available on the pathogenesis of this ALL subtype. The heterogeneous distribution of patients based on relapse rates and response to therapy indicates an important underlying mechanism that determines patient prognosis.

Through Low Density Array miRNA profiling of patient samples, 50 miRNAs were differentially expressed with significance at pvalues less than 0.05. 49 miRNAs were up regulated and only 1 miRNA was down regulated in MH normal karyotype patients, and of the 49 up regulated miRNAs, hsa-miR-221/222 had the highest levels of up-regulation. Hierarchical average clustering separated the patients into their respective ML and MH groups, and validation of miRNA expression in an enlarged group of ML(n=18) and MH(n=15) patients showed that miR-221/222 were over expressed

in MH patients with pvalues less than 0.0001 , thereby providing experimental support for the use of miRNA expression as a means of complementing MRD for patient stratification.

Stable over expression of miR-221/222 showed decreased sensitivity to glucocorticoid treatment in the form of higher viability, lower caspase activity and increased proliferation with a approximately 20% corresponding increase in S phase cells over the negative control.

NLK is a predicted target of miR-221/222 and in western blotting, was reduced in cell lines over expressing miR-221/222 and validation of NLK mRNA in patient samples showed that ML expression was 3-fold greater than MH with pvalue of 0.0042.

In summary, miR-221/222 is a factor in mediating the heterogeneous responses of Normal Karyotype B-cell precursor ALL patients to glucocorticoid treatment, with the over expression associated with high MRD measurements and poor prognosis. Experimental evidence showed that NLK is a protein target of miR-221/222 and is correspondingly down regulated in cells over expressing miR-221/222.

3.2. Alternative Therapeutics

With the identification of the miRNAs involved in mediating chemoresistance, as well as its protein targets in Normal Karyotype B-cell precursor ALL, alternative therapeutics may be

exploited as a cure, or as an adjuvant in complementing standard chemotherapy protocols.

Histone deactylase inhibitors[32] (HDi) were reportedly capable of augmenting the therapeutic effects of several drugs used in chemotherapy, by facilitating the apoptosis process. This adjuvant effect allows for lower doses of drugs to be used in patients who respond well to chemotherapy, with the added benefit of reduced side effects. And in patients who do not respond well or have poor prognosis, a greater therapeutic effect may be achieved with the standard maximal dose allowed. Previous studies have implicated NLK in apoptosis induction[29,30], and so NLK may be used as an alternative apoptosis-inducing agent. As reviewed by Li[33] et al, natural agents like cucurmin and isoflavone are being evaluated for their targeted effects in abrogating specific miRNA over expression which contributes to chemoresistance, and inhibitors of miR-221/222 could also be exploited to sensitize cancer cells to chemotherapeutic drugs, as reported by Garofalo[24] et al and Zhao[34] et al. Hence, there are still alternative therapeutics in existence to counter chemoresistance in cancer cells.

3.3. Pathway Identification

The next step forward is to elucidate the pathway that is regulated by NLK. NLK is localized in the nucleus[35] and is known to phosphorylate CREB binding protein[31] (CBP), and phosphorylated CBP[36,41] is an important factor in the transcription complex[37] of

numerous pathways that includes the glucocorticoid receptor pathway[38]. Glucocorticoid receptors exist as a multi-protein complex[39] localized in the cytoplasm, and glucocorticoids function by binding to such protein complexes, after which the glucocorticoid receptors dissociate from the complex and translocate to the nucleus. Within the nucleus, the glucocorticoid receptors associate with P300, acetyl-CBP, PCAF and SRC that function as coactivators[37] of transcription. This transcription complex recognizes and binds to glucocorticoid receptor elements (GRE), and initiates the transcription of glucocorticoid target genes that in turn drives a whole host of apoptosis mechanisms that result in cell death.

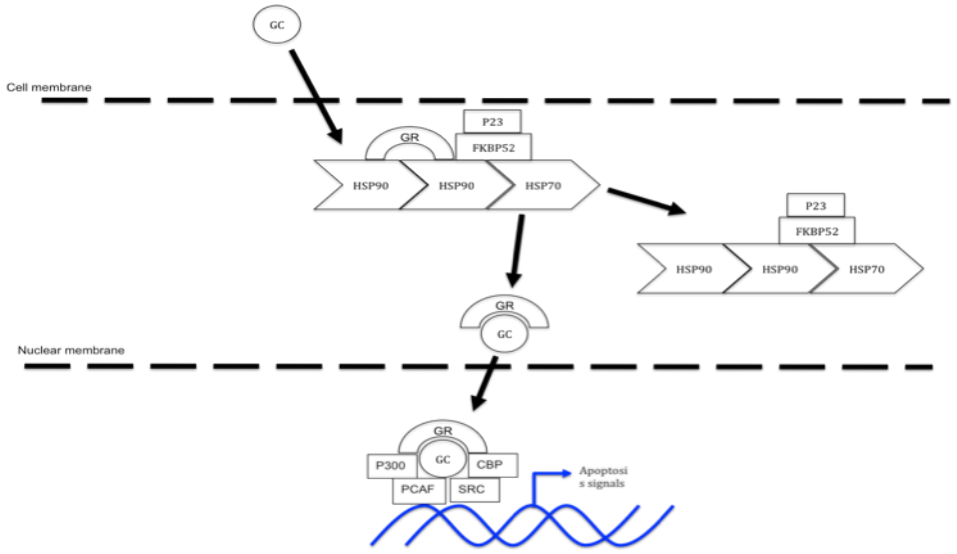

Figure 14. Schematic showing how glucocorticoids interact with glucocorticoid receptors and to initiate apoptosis.
Adapted from QIAGEN website
http://www.sabiosciences.com/pathway.php?sn=Glucocorticoid_Receptor_Signaling

Initial western blotting data showed that acetyl-CBP levels varied in accordance with reduction of NLK and over-expression of miR-221/222 (Figure 11). And as a consequence, the activity of the glucocorticoid receptor pathway is possibly attenuated due to the reduction of acetyl-CBP, resulting in reduced apoptotic activity in the presence of glucocorticoids.

A recent study by Mullighan[40] et al, analyzed the sequencing data of a select group of 300 genes in ALL patients. Their group identified somatic deletions and/or substitutions in cotransactivators CBP and the glucocorticoid receptor NCOR1 with a frequency of 18.3% in the relapse patients. The mutations were present in the histone acetyltransferase domains of the genes and were detected at diagnosis or relapse. The mutations produced truncated or deleterious proteins and resulted in aberrant transcription of CBP and glucocorticoid target genes, and with several mutations acquired at relapse similarly detected at diagnosis, they suggested that such mutations may confer resistance to therapy. Therefore, their study reinforces the notion that CBP is an important regulator of sensitivity to chemotherapy and that histone modification is essential to the induction of apoptosis by the glucocorticoid receptor pathway.

In conclusion, NLK interaction with CBP is biologically important in mediating apoptosis due to glucocorticoid stimulation of the glucocorticoid receptor pathway, while over expression of miR-

221/222 down regulate NLK levels to indirectly dysregulate the glucocorticoid pathway. Hence, further experimentation is required to validate that the NLK-CBP interaction affects causality of chemoresistance in B-cell precursor ALL.

3.4 References.

1. Graux C. Biology of acute lymphoblastic leukemia (ALL): clinical and therapeutic relevance. *Transfusion and Apheresis Science.* 2011; 44: 183-9.

2. Pui CH, Relling MV, Downing JR. Acute lymphoblastic leukemia. *N Engl J Med.* 2004; 350: 1535-48.

3. Puil L, Liu J, Gish G, Mbamalu G, Bowtell D, Pelicci PG*, et al*. Bcr-Abl oncoproteins bind directly to activators of the Ras signalling pathway. *EMBO J.* 1994; 13: 764-73.

4. Robert Jr L, Van Etten RA. P210 and P190(BCR/ABL) induce the tyrosine phosphorylation and DNA binding activity of multiple specific STAT family members. *The Journal of Biological Chemistry.* 1996; 271: 31704-10.

5. Cortez D, Reuther G, Pendergast AM. The Bcr-Abl tyrosine kinase activates mitogenic signaling pathways and stimulates G1-to-S phase transition in hematopoietic cells. *Oncogene.* 1997; 15: 2333-42.

6. Speck NA, Gilliland DG. Core-binding factors in haematopoiesis and leukaemia. *Nature Reviews Cancer.* 2002; 2: 502-13.

7. Hiebert SW, Sun W, Davis JN, Golub T, Shurtleff S, Buijs A*, et al*. The t(12;21) translocation converts AML-1B from an activator to a repressor of transcription. *Mol Cell Biol.* 1996; 16: 1349-55.

8. Gilliland DG, Griffin JD. The roles of FLT3 in hematopoiesis and leukemia. *Blood.* 2002; 100: 1532.

9. Armstrong SA, Kung AL, Mabon ME, Silverman LB, Stam RW, Den Boer ML*, et al*. Inhibition of FLT3 in MLL. Validation of a therapeutic target identified by gene expression based classification. *Cancer Cell.* 2003; 3: 173-83.

10. Omura-Minamisawa M, Diccianni MB, Batova A, Chang RC, Bridgeman LJ, Yu J*, et al*. Universal inactivation of both p16 and p15 but not downstream components is an essential event in the

pathogenesis of T-cell acute lymphoblastic leukemia. *Clinical Cancer Research.* 2000; 6: 1219-28.

11. Pui C-, Carroll WL, Meshinchi S, Arceci RJ. Biology, risk stratification, and therapy of pediatric acute leukemias: an update. *Journal of Clinical Oncology : official journal of the American Society of Clinical Oncology* 2011; 29: 551-65.

12. Flohr T, Schrauder A, Cazzaniga G, Panzer-Grumayer R, van der Velden V, Fischer S*, et al*. Minimal residual disease-directed risk stratification using real-time quantitative PCR analysis of immunoglobulin and T-cell receptor gene rearrangements in the international multicenter trial AIEOP-BFM ALL 2000 for childhood acute lymphoblastic leukemia. *Leukemia.* 2008; 22: 771-82.

13. Cazzaniga G, Biondi A. Molecular monitoring of childhood acute lymphoblastic leukemia using antigen receptor gene rearrangements and quantitative polymerase chain reaction technology. *Haematologica.* 2005; 90: 382-90.

14. Szczepana T, Flohr T, van der Velden VHJ, Bartram CR, van Dongen JJM. Molecular monitoring of residual disease using

antigen receptor genes in childhood acute lymphoblastic leukaemia. *Best Practice & Research Clinical Haematology.* 2002; 15: 37-57.

15. Szczepana T. Why and how to quantify minimal residual disease in acute lymphoblastic leukemia? *Leukemia.* 2007; 21: 622-6.

16. Panzer-Grumayer ER, Schneider M, Panzer S, Fasching K, Gadner H. Rapid molecular response during early induction chemotherapy predicts a good outcome in childhood acute lymphoblastic leukemia. *Blood.* 2000; 95: 790-4.

17. Coustan-Smith E, Sancho J, Hancock ML, Boyett JM, Behm FG, Raimondi SC*, et al*. Clinical significance of minimal residual disease in childhood acute lymphoblastic leukemia. *Blood.* 2000; 96: 2691-6.

18. Marshall GM. Importance of Minimal Residual Disease Testing During the Second Year of Therapy for Children With Acute Lymphoblastic Leukemia. *Journal of Clinical Oncology.* 2003; 21: 704-9.

19. Bartel DP. MicroRNAs: target recognition and regulatory functions. *Cell.* 2009; 136: 215-33.

20. Cimmino A. miR-15 and miR-16 induce apoptosis by targeting BCL2. *Proceedings of the National Academy of Sciences.* 2005; 102: 13944-9.

21. 18. Garzon R, Heaphy CEA, Havelange V, Fabbri M, Volinia S, Tsao T*, et al*. MicroRNA 29b functions in acute myeloid leukemia. *Blood.* 2009; 114: 5331-41.

22. Visone R, Veronese A, Rassenti LZ, Balatti V, Pearl DK, Acunzo M*, et al*. miR-181b is a biomarker of disease progression in chronic lymphocytic leukemia. *Blood.* 2011; 118: 3072-9.

23. Bousquet M, Harris MH, Zhou B, Lodish HF. MicroRNA miR-125b causes leukemia. *Proceedings of the National Academy of Sciences.* 2010; 107: 21558-63.

24. Garofalo M, Di Leva G, Romano G, Nuovo G, Suh S, Ngankeu A*, et al*. miR-221&222 regulate TRAIL resistance and enhance tumorigenicity through PTEN and TIMP3 downregulation. *Cancer Cell.* 2009; 16: 498-509.

25. Brioschi M, Fischer J, Cairoli R, Rossetti S, Pezzetti L, Nichelatti M*, et al*. Down-regulation of microRNAs 222/221 in acute myelogenous leukemia with deranged core-binding factor subunits. *Neoplasia.* 2010; 12: 866.

26. Frenquelli M, Muzio M, Scielzo C, Fazi C, Scarfo L, Rossi C*, et al*. MicroRNA and proliferation control in chronic lymphocytic leukemia: functional relationship between miR-221/222 cluster and p27. *Blood.* 2010; 115: 3949-59.

27. Felicetti F, Errico MC, Bottero L, Segnalini P, Stoppacciaro A, Biffoni M*, et al*. The promyelocytic leukemia zinc finger-microRNA-221/-222 pathway controls melanoma progression through multiple oncogenic mechanisms. *Cancer Res.* 2008; 68: 2745-54.

28. Cui G, Li Z, Shao B, Zhao L, Zhou Y, Lu T*, et al*. Clinical and biological significance of nemo-like kinase expression in glioma. *Journal of clinical neuroscience.* 2011; 18: 271-5.

29. Emami KH, Brown LG, Pitts TEM, Sun X, Vessella RL, Corey E. Nemo-like kinase induces apoptosis and inhibits androgen

receptor signaling in prostate cancer cells. *Prostate.* 2009; 69: 1481-92.

30. Yasuda J, Tsuchiya A, Yamada T, Sakamoto M, Sekiya T, Hirohashi S. Nemo-like kinase induces apoptosis in DLD-1 human colon cancer cells. *Biochem Biophys Res Commun.* 2003; 308: 227-33.

31. Yasuda J, Yokoo H, Yamada T, Kitabayashi I, Sekiya T, Ichikawa H. Nemo-like kinase suppresses a wide range of transcription factors, including nuclear factor-kB. *Cancer Science.* 2004; 95: 52-7.

32. Kouraklis G. HDAC inhibitors in leukemia: current status and perspectives. *Leuk Res.* 2009; 33: 207-8.

33. Li Y, Kong D, Wang Z, Sarkar FH. Regulation of microRNAs by natural agents: an emerging field in chemoprevention and chemotherapy research. *Pharm Res.* 2010; 27: 1027-41.

34. Zhao J-, Lin J, Yang H, Kong W, He L, Ma X*, et al*. MicroRNA-221/222 negatively regulates estrogen receptor alpha and is

associated with tamoxifen resistance in breast cancer. *The Journal of biological chemistry.* 2008; 283: 31079-86.

35. BROTT BK, PINSKY BA, ERIKSON RL. Nlk is a murine protein kinase related to Erk MAP kinases and localized in the nucleus. *Proc Natl Acad Sci USA.* 1998; 95: 963–968.

36. Zanger K, Radovick S, Wondisford FE. CREB binding protein recruitment to the transcription complex requires growth factor-dependent phosphorylation of its GF box. *Mol Cell.* 2001; 7: 551-8.

37. Vo N, Goodman RH. CREB-binding protein and p300 in transcriptional regulation. *The Journal of biological chemistry.* 2001; 276: 13505-8.

38. Schoneveld O, Gaemers I, LAMERS W. Mechanisms of glucocorticoid signalling. *Biochimica et Biophysica Acta (BBA) - Gene Structure and Expression.* 2004; 1680: 114-28.

39. Greenstein S, Ghias K, Krett NL, Rosen ST. Mechanisms of glucocorticoid-mediated apoptosis in hematological malignancies. *Clinical Cancer Research.*2002; 8: 1681-94.

40. Mullighan CG, Zhang J, Kasper LH, Lerach S, Payne-Turner D, Phillips LA*, et al*. CREBBP mutations in relapsed acute lymphoblastic leukaemia. *Nature* 2011; 471: 235-9.

41. Ait-Si-Ali S, Carlis D, Ramirez S, Upegui-Gonzalez L, Duquet A, Robin P*, et al*. Phosphorylation by p44 MAP Kinase/ERK1 Stimulates CBP Histone Acetyl Transferase Activity in Vitro. *Biochem Biophys Res Commun* 1999; **262**: 157-62.

3.5 **Supplemental Information**

Patient Datasheet

patient	WBC	immunophenotype	t(4;11)	t(t9;22)	t(12;21)	DNA index	mrd_M1_d33	mrd_M2_d33	mrd_M1_d78	mrd_M2_d78
ML01	3150	cALL	NEG	NEG	NEG	1.22	0.0E+00	0.0E+00	0.0E+00	0.0E+00
ML02	81300	pre-B	NEG	NEG	NEG	1	0.0E+00	0.0E+00	0.0E+00	0.0E+00
ML03	22710	pre-B	NEG	NEG	NEG	0.898	0.0E+00	0.0E+00	0.0E+00	0.0E+00
ML04	8800	pre-B	NEG	NEG	NEG	1	0.0E+00	0.0E+00	0.0E+00	0.0E+00
ML05	130270	pre-B	NEG	NEG	NEG	1	0.0E+00	0.0E+00	0.0E+00	0.0E+00
ML06	34700	pre-B	NEG	NEG	NEG	1	0.0E+00	0.0E+00	0.0E+00	0.0E+00
ML07	2520	cALL	NEG	NEG	NEG	1	0.0E+00	0.0E+00	0.0E+00	0.0E+00
ML08	5200	cALL	NEG	NEG	NEG	1.069	0.0E+00	0.0E+00	0.0E+00	0.0E+00
ML09	4180	cALL	NEG	NEG	NEG	1	0.0E+00	0.0E+00	0.0E+00	0.0E+00
ML10	16030	pre-B	NEG	NEG	NEG	1	0.0E+00	0.0E+00	0.0E+00	0.0E+00
ML11	33700	cALL	NEG	NEG	NEG	1	0.0E+00	0.0E+00	0.0E+00	0.0E+00
ML12	13700	pre-B	NEG	NEG	NEG	1	0.0E+00	0.0E+00	0.0E+00	0.0E+00
ML13	11000	cALL	NEG	NEG	NEG	1.088	0.0E+00	0.0E+00	0.0E+00	0.0E+00
ML14	17900	pre-B	NEG	NEG	NEG	1	0.0E+00	0.0E+00	0.0E+00	0.0E+00
ML15	11410	cALL	NEG	NEG	NEG	No data	0.0E+00	0.0E+00	0.0E+00	0.0E+00
ML16	6700	pre-B	NEG	NEG	NEG	1.19	0.0E+00	0.0E+00	0.0E+00	0.0E+00
ML17	4300	cALL	NEG	NEG	NEG	1.219	0.0E+00	0.0E+00	0.0E+00	0.0E+00
ML18	273000	pre-B	NEG	NEG	NEG	1	0.0E+00	0.0E+00	0.0E+00	0.0E+00
MH01	12880	cALL	NEG	NEG	NEG	1	2.4E-02	3.1E-02	7.4E-04	8.0E-04
MH02	5720	cALL	NEG	NEG	NEG	1.218	1.3E-03	1.4E-03	6.4E-04	4.6E-04
MH03	3550	cALL	NEG	NEG	NEG	1	5.0E-05	0.0E+00	0.0E+00	0.0E+00
MH04	31600	cALL	NEG	NEG	NEG	1	8.8E-04	9.9E-04	5.7E-05	1.9E-04
MH05	12570	pre-B	NEG	NEG	NEG	No data	6.2E-05	0.0E+00	1.0E-05	0.0E+00
MH06	46380	cALL	NEG	NEG	NEG	1	2.3E-03	1.8E-03	3.4E-05	1.2E-05
MH07	2400	cALL	NEG	NEG	NEG	1	0.0E+00	0.0E+00	1.0E-04	1.0E-04
MH08	7200	cALL	NEG	NEG	NEG	1.329	1.7E-03	1.3E-03	0.0E+00	0.0E+00
MH09	22470	pro-B	NEG	NEG	NEG	1	2.2E-02	1.2E-02	7.7E-04	7.1E-04
MH10	68650	cALL	NEG	NEG	NEG	1	7.4E-02	4.8E-02	5.0E-05	0.0E+00
MH11	4500	cALL	NEG	NEG	NEG	No data	7.6E-02	6.2E-02	7.2E-03	2.3E-03
MH12	3390	cALL	NEG	NEG	NEG	1.161	6.9E-03	4.1E-03	1.7E-04	0.0E+00
MH13	11500	cALL	NEG	NEG	NEG	1	1.5E-02	2.1E-02	7.4E-04	9.8E-04
MH14	9160	cALL	NEG	NEG	NEG	1	3.5E-02	3.0E-02	6.6E-03	7.0E-03
MH15	86780	cALL	NEG	NEG	NEG	1	3.2E-03	2.1E-03	1.9E-03	7.4E-04

Acknowledgements.

I would like to extend my appreciation to the following people:

Prof Andrea Biondi for accepting me into the DIMET programme, and giving me the opportunity to be in Italy.

Dr Giovanni Cazzaniga for being my supervisor and providing invaluable guidance along the way.

Prof Carlo Croce for allowing me to be on attachment in his lab at Ohio USA.